NGU Report 2010.018

Results of borehole logging in well LYB CO2, Dh4 of 2009, Longyearbyen, Svalbard

Geological Survey of Norway
NO-7441 Trondheim, Norway
Tel.: 47 73 90 40 00
Telefax 47 73 92 16 20

REPORT

Report no.: 2010.018	ISSN 0800-3416	Grading: Open

Title:
Results of borehole logging in well LYB CO2, Dh4 of 2009, Longyearbyen, Svalbard

Authors: Harald Elvebakk	Client: UNIS
County: Svalbard	Commune: Longyearbyen
Map-sheet name (M=1:250.000)	Map-sheet no. and -name (M=1:50.000)
Deposit name and grid-reference: LYB CO2 Dh4-2009 UTM 33X, E518889 N8681108	Number of pages: 35 Price (NOK): 210.- Map enclosures:

Fieldwork carried out: 10.10.09 – 12.10.09 02.12.09	Date of report: 11.03.2010	Project no.: 322300	Person responsible: Jan S. Rønning

Summary:

NGU has carried out borehole logging in well LYB CO2 Dh4, in Adventdalen 5 km outside Longyearbyen. The well was drilled to locate deep sandstone formations that may be used to store CO_2. The project "Longyearbyen CO_2 Lab" of UNIS and partners, will use the test site as laboratory for injection, storing and monitoring CO_2 in the underground. The well was drilled full coring telescope operation to 970 m and was successful in that it cored Late Triassic sandstones that also show injectivity.

Logging parameters were temperature, fluid conductivity, natural gamma, rock resistivity, seismic velocity, caliper, relative density and borehole deviation. The well was also inspected by acoustic televiewer to map fractures. Because of a cased wellbore and the small borehole diameter in the deepest part, the entire borehole could not be logged.

The results show good correlation between the geophysical logs and the lithological units. Sandstones are indicated with low gamma radiation and increasing seismic velocity and apparent resistivity. Acoustic televiewer interpretation shows that some of the sandstones are highly fractured, which is confirmed by lowered seismic velocity and resistivity. Cap rock silt- and mudstones are fractured but the fractures do not influence strongly on the seismic velocity and resistivity log. In sum, this might indicate that the fractures in the sandy layers are open and water filled, whereas fractured siltstone is tight.

Keywords: Geophysics	Borehole logging	Resistivity
Seismic velocity	Temperature	Fluid conductivity
Natural Gamma	Deviation	Density
Acoustic Televiewer		Scientific Report

CONTENTS

FIGURES

TABLES

APPENDIX

1. INTRODUCTION

This report is a continuation of NGU Report 2008.054 (covering wells Dh1 and Dh2) and describes the result of the geophysical logging in well No.4 in the Longyearbyen CO_2 lab project which was stated in 2007.

In Longyearbyen, Svalbard, all electrical energy is produced by a coal combusting power plant. The power plant is emitting about 80 000 tons of CO_2 per year. A research programme initiated by the University Centre in Svalbard (UNIS) has a vision to make Longyearbyen free of man-made CO_2. The Longyearbyen CO_2 Lab main goal is to study the injection, storing and monitoring the CO2 in a suitable aquifer. UNIS also wants to develop high level educational courses as part of the project.

The first phase in the project has been to identify a deep sandstone formation below the surface near Longyearbyen which is suitable for injection and storing of CO_2. Two wells were drilled in 2007 close to the airport. Significant problems caused by a 25 m thick fault zone of highly fractured shale at 450 m depth caused stability problems, and in the end stopped the drilling at ca. 870 m depth in well Dh2-CO_2-07. The well failed to reach the main reservoir that is prognosed to be in Late Triassic sandstone. Previous to this well, a well Dh1-CO_2-07 was drilled to 518 m depth. Also this well failed for the same reason. Both wells were logged by NGU down to the fault zone at 440 m depth (Elvebakk 2008).

A third well was drilled in August-October 2008, a few kilometers into the Advent Valley, approximately 5 km from Longyearbyen. The well reached 403 m coring the cap rocks. Due to the stability problems in the fault zone the drilling failed to get further down.

In August - December 2009 a well number 4 was drilled in Adventdalen 45 m from Dh 3. After significant upgrading of drilling equipment, and by reducing well bore diameter at deeper levels and cementing successive casings, the well reached 970 m. The deepest 100 m were drilled using a 46 mm drill rod. This small dimension reduced the accessibility in the well for the logging tools.

The borehole logging was performed in two parts (periods). The upper 440 m was not fully logged because of the cemented casing in this part of the well. The logging parameters were temperature, fluid conductivity, natural gamma, rock resistivity, seismic velocity, caliper, relative density and borehole deviation. Acoustic telewiever (HIRAT, High Resolution Acoustic Televiewer) was run in one part of the borehole, 440 m – 700 m.

The logging was carried out 10.10.09 – 12.10.09 and 02.12.09 by Harald Elvebakk, NGU, assisted by the drilling crew from LNS Spitsbergen.

2. BOREHOLE LOCATION AND LOGGING PERFORMANCE.

The Dh4-CO_2 well is located in Adventdalen, close to the former Auroral Observatory approximately 5 km from Longyearbyen, see figure 1.Well data are shown in table 1.

Figure 1. Borehole location in Adventdalen. The blue tower hosts the drill rig.

Tabel 1. Well data Dh4-CO2-09

Well	**Drilled depth(m)**	**Logging depth (m)**	**Drilling finished**	**Logging date**	**UTM-East 33X**	**UTM-North 33X**
LYB CO2 Dh4-2009	790	440-790	10.10.09	10-12.10.09	518889	8681108
LYB CO2 Dh4-2009	870-970	790-915	27.11.09	02.12.2009	518889	8681108

Four different well diameters were used. In the upper 440 m a HQ core bit (OD 96 mm) was used. The HQ rod was cemented down to this depth which reduced the logging parameters to only temperature and gamma radiation. From 440 m to 790.5 m the NQ (76 mm) rod was used. In this section the logging was performed in the first logging period, 10.10.-12.10.09. During the logging a rock fall at about 710 m depth blocked the bore hole thereby cancelling caliper, density and HIRAT data between 705 and 790 m.

Drilling from 790 m was performed by the BQ rod (60 mm).This drill string locked at 870 m and could not be moved. After discussions it was decided to continue the drilling with the 46 mm string from 870 m, leaving the BQ rod in the borehole . Due to geological information and two interesting water injection tests, the drilling was stopped at 970 m. Logging in the deepest section (46 mm), 870 – 970 m, could only be done with the thinnest probes, temperature/gamma/conductivity and caliper. Nevertheless the temperature probe stopped at about 915 m in the narrow bore hole. This probe was run from the surface. Caliper was run from 870 to 915 m. The density probe could have been run, but the risk for losing the probe with a radioactive Cs gamma source in the bore hole was considered too high.

3. LOGGING PARAMETERS

The logging parameters monitored by various tools were temperature, fluid conductivity, natural gamma, rock resistivity, seismic velocity, caliper, relative density and borehole deviation. The logging equipment is produced by Robertson Geologging Ltd. (http://www.geologging.com/).
The caliper and density probe belonged to SNSK. Short descriptions for the other probes (NGU) can be found on NGU's web site:
http://www.ngu.no/no/hm/Norges-geologi/Geofysikk/Borehullsgeofysikk/

Detailed exploration of the tables in the Appendix can also be found on this web site.

3.1 Temperature

Temperature measurements should ideally be performed some time after the drilling stops, since the energy from the drilling process (hot drilling fluid, rock crushing, and friction) will increase the temperature in the borehole. Stabilizing the temperature may take several weeks depending on the drilling method and borehole diameter. Commonly the upper 25-30 m of a borehole will be influenced by seasonal variations in the near surface temperature. From the temperature log the temperature gradient (^{o}C/km) can be calculated. Local changes in the gradient may indicate fractures and related inflow (or outflow) of water.

3.2 Conductivity

The fluid conductivity (µS/cm) depends on the fluid salinity. The conductivity measurements can identify zones of water in-flow/out-flow and locate zones of different water quality. The measured values are temperature compensated to a reference temperature of 25 ^{o}C. In the CO_2 boreholes the conductivity is very high, caused both by the saline drilling water and by saline groundwater.

3.3 Natural Gamma

The natural gamma log (cps) is useful for geological mapping along walls of a borehole. All rocks contain small quantities of radioactive material, in that certain minerals contain trace amounts of Uranium and Thorium. Potassium-bearing minerals (most common) will include traces of a radioactive isotope of Potassium (K_{40}). Natural gamma measurements are useful because the radioactive elements are concentrated in certain rock types, e.g. clay, shale and granite, and depleted in others, e.g. sandstone and coal. The unit (cps) is in API standard units which mean that data can be compared to other measurements performed with the same standard.

3.4 Resistivity

Resistivity logging in boreholes is extensively used in hydrocarbon exploration of sedimentary rocks both to identify lithological boundaries and to estimate the rock porosity. The resistivity depends on porosity and fractures (water content), content of electronic conductive minerals such as sulphides, oxides and graphite and clay. Saline pore water will influence on the apparent resistivity. The resistivity is measured using two configurations, Short Normal (SN) and Long Normal (LN). The resistivity data are processed by using a program that corrects borehole resistivity logging data for the influence of the borehole liquid, borehole diameter and probe size (Thunehed & Olsson 2004). The porosity is calculated using the measured resistivity and Archie's law (Archie 1942). Archie's law was found to be correct for porous sandstones with uniform grain size. If other parameters than the porosity (e.g. electronic conductive minerals, fractures) influence on the resistivity, the calculated porosity using Archie's law will be wrong.

3.5 Seismic velocity

The sonic probe has one transmitter and two receivers separated by 30.4 cm, that records the full sonic wave-train at both receivers simultaneously and also the velocity of the first arrival. Both P-velocity (compression) and S-velocity (shear wave) are calculated every 20 cm. Data are filtered using a running average filter over 0.8 m. The first arrival of the P-wave is quite easy to pick while the arrival of the S-wave is more indistinct. P-velocity (formation velocity) is used for lithological identification and fracture mapping. Data processing is done by using software from ALT (ALT 2006).

3.6 Caliper

The three-arm caliper probe (from SNSK) provides a single continuous log of borehole diameter. The applications of the caliper measurements are location of cracks, fissures, caving, faulting and casing breaks. It is also used for correction of other logs affected by borehole diameter (resistivity, density).

3.7 Density (qualitative measurements)

The trisonde density probe (from SNSK) is a convenient alternative to the standard RG sidewall density probe whenever borehole diameter is restricted and qualitative density measurements are sufficient. The trisonde log can be used for lithological identification, bed thickness and boundary location based on relative changes in the density.

3.8 Deviation

The RG verticality probe provides accurate, continuous measurements of borehole inclination and direction. The probe includes a triaxial magnetometer for measuring the borehole orientation (azimuth accuracy +/- 1^{o}) and three accelerometers to measure inclination (accuracy +/- 0.5^{o}). From this the East and North deviation components are calculated.
The azimuth measurements will be wrong inside the casing because of the magnetic properties of the casing.

3.9 Acoustic televiewer

The HIRAT (also named BHTV, Bore Hole TeleViewer) sonde uses a fixed acoustic transducer and rotating mirror system to acquire 2-way travel-time and amplitude of the acoustic signal reflected back to the transducer from a spiral trajectory on the borehole wall. From this an image of the borehole wall are constructed using both the travel-time and amplitude signal. Pixel size at the borehole wall is approximately 1 x 1 mm using the highest resolution (360 shots per revolution).

Fracture study through processing aims to identify geometric sets of fractures/veins, and then estimate variations in mean dip and frequency within the sets and lines of intersection among the sets, with depth. In sedimentary rocks, the structural interpretation aims to extract formation dip and to identify geological structures such as unconformities, folds and faults, from the distribution and orientation of dips assigned to bedding.

Digitalizing the observed features on the well bore image creates strike and dip of identified structures which can be presented in fracture stereograms, rose diagrams, fracture frequency histograms, and thickness calculations of beds, bands and fractures. The deviation of the borehole is also calculated.

4. RESULTS

Logging was performed in two periods, 10.-12.10.2009 and 2.12.2009. All parameters were logged during the first period down to 790 m, for some tools to700 m. Only temperature, fluid conductivity and natural gamma were logged from the surface due to the cased well down to 440 m. P-velocity, S-velocity and Resistivity were logged from 440 m – 790 m, Caliper and Density from 440 m – 705 m. A rock fall blocked the bore hole at 710 m before the latter two logs were run.

The calculated porosity is very high. The porosity is calculated using the resistivity, see chapter 3.4. The measured resistivity is very low, especially in the claystones. Clay minerals contribute to the measured electric conductivity and Archie*s law fails. This results in a very high porosity which obviously is wrong, and the porosity data are not included in the logs.

The logs are presented as continuous plots including several parameters:

- P- and S- velocity, Natural Gamma, Resistivity, Thermal gradient, Density and Caliper.
- Temperature, thermal gradients (20 m and 100 m depth intervals) for both periods.
- Temperature, fluid conductivity,
- Deviation, North- and East projection and horizontal projection (direction)
- Acoustic televiewer, fracture stereogram and fracture frequency histograms.

The sonic data were processed using the WellCad software from ALT (ALT 2006). The resistivity data were processed by using a program that corrects borehole resistivity logging data for the influence of the borehole liquid conductivity, borehole diameter and probe size. (Thunehed & Olsson 2004).

The thermal gradients are calculated using running least-squares gradients of a straight line with depth intervals of 20 m and 100 m. In such analysis the 20 m interval is more sensitive to local variations in the temperature.

4.1 Dh4-CO_2-09, P- and S- velocity, Natural Gamma, Resistivity, Thermal gradient, Density and Caliper.

The well reached the main reservoir (sandstone) and the total depth of the well is 970 m.

Figure 2 shows the logs of P-velocity, S-velocity, natural gamma, resistivity, thermal gradient, caliper and qualitative density for the section 440 m – 790 m. Natural gamma and temperature are logged from the surface to 900 m. The data quality is quite good for all logs. The gamma radiation data are corrected due to the casing which will attenuate some part of the radiation. The temperature is measured 5 days after ended drilling and the influence from drilling operation is expected to be small, see later chapter 4.3. Different stratigraphic units (formations) can be recognized on the gamma log which covers almost the complete bore hole. This is shown in figure 3 which includes a stratigraphic log (Atle Mørk, pers. com.).

Figure 4 shows logs below 440 m depth. Figure 5 shows the same logs now including the main lithological units from the sediment logs (Atle Mørk and UNIS pers. com.).

The P-velocity log is indicating P-velocities of 3000 – 4500 m/s. Average velocities for the main units are: sandstone – 4200 m /s and silt/mudstone – 3350 m/s. This is in the range of normal velocities for sandstone, silt-and mudstone.

Normal values for sandstones is in the range of some 10 ohmm to several 10 000 ohmm (Schön 2004). Measured values are 20 – 30 ohmm in the siltstone and 50 - 100 ohmm in the sandstone. This is lower than the resistivity values in Dh1 and Dh2 and can be explained by the very high conductivity in the water. In Dh1 and Dh2 the fluid conductivity was about 10000 µS/cm, while the conductivity in Dh4 was 20000 – 50000 µS/cm. Another reason could be that the logged section in Dh4 is deeper in the stratigraphy containing rocks with other properties.

The resistivity data are corrected due to the borehole water conductivity, which is saline water. However, in this case the pore water is most likely saline groundwater and this will also have an influence on the measured values. By using Archie's law the formation resistivity ρ_o can be calculated from the porosity, Φ, pore water resistivity, ρ_w. and cementation exponent, m. (Archie 1942).

$$\rho_o / \rho_w = 1/ \Phi^m$$

If we assume a porosity of 10 %, pore water conductivity of 25 000 µS/cm and m equal to 2, the calculated formation resistivity will be 40 ohmm. This fits well with the logged values, 20 – 100 ohmm. The important issue here, however, is how the resistivity varies due to the changing lithology.

The gamma log indicates changes in the lithology. The caliper log indicates fractures, but can also be related to small changes in the borehole diameter caused by variations in the rock hardness. In this way the formation thickness is indicated. For the density log, although this tool gives a qualitative density measurement, the layer thicknesses are indicated. The density is also influenced by changes in borehole diameter.

In the following, some examples of log interpretations are described (units are marked with different colors in figure 5).

440 – 545 m : Layers of siltstone with small amount of sand (UNIS litholog). The P-velocity is very low down to 490 m depth, 3000 m/s, likewise the S-velocity, 1600 – 2000 m/s. The resistivity is low, 25 ohmm and the gamma radiation is quite constant 130-140 cps. A slight increase in P-velocity and resistivity from 500 m is probably caused by an increase in the amount of sand. The caliper log shows an increased diameter from 535 to 440 m. The fracture frequency is high, see later (acoustic televiewer). The density log shows an increase in cps in the same section. This increase is probably caused by the increased diameter. At 535 – 545 m depth there is a distinct increase in the gamma radiation and the resistivity while the P-velocity decreases. This is uniform siltstone (from UNIS litholog) and the changes in these parameters are difficult to explain.

545 – 590 m : Sandy mudstone/siltstone. The amount of sand is 30-50 % (UNIS litholog). P- and S-velocity increase to 4000-4200 m/s and 2300 – 2600 m/s. The resistivity is 50-70 ohmm except for low values locally at 575 m depth. The gamma radiation decreases due to the increased amount of sand. The borehole diameter is stable except a small increase at 565-575 m depth probably caused by fractures.

590 – 670 m : Siltstone. The P- and S-velocity decreases in this unit which is normal. The resistivity increases to 75 – 100 ohmm at 610-630 m depth. In the same depth interval the gamma radiation increases to 175 cps and the relative density (in cps) has a slight increase (slight decrease in real density). The higher resistivity should indicate more sand, but the higher gamma radiation and lower P-velocity point in the opposite direction. This section of the borehole is highly fractured which normally means lowered resistivity. Therefore it’s difficult to explain the high resistivity and high gamma. The strong decrease in resistivity from 630 m depth is caused by highly fractured rock which is confirmed by the caliper log and acoustic televiewer.

670 – 680 m : Sandstone and conglomerate. This section belongs to the Wilhelmøya Subgroup in De Geerdalen Formation. A conglomerate, 675-678 m, is indicated by low seismic velocity, low gamma and low resistivity (SN).

680 – 765 m : Alternating layers of sandstone, siltstone and silt-mudstone with no special events on the logs. A very high value of P- and S-velocity at 687 m is probably caused by a thin layer of massive sandstone.

765 – 800 m : Sandstone indicated by strong increase in the resistivity, this is massive sandstone. P-velocity is 4200 – 4400 m/s.

Below 800 m : Below 800 m the only logged parameters are gamma radiation, temperature and fluid conductivity. Variations in the gamma radiation indicate alternating layers of sandstone/siltstone.

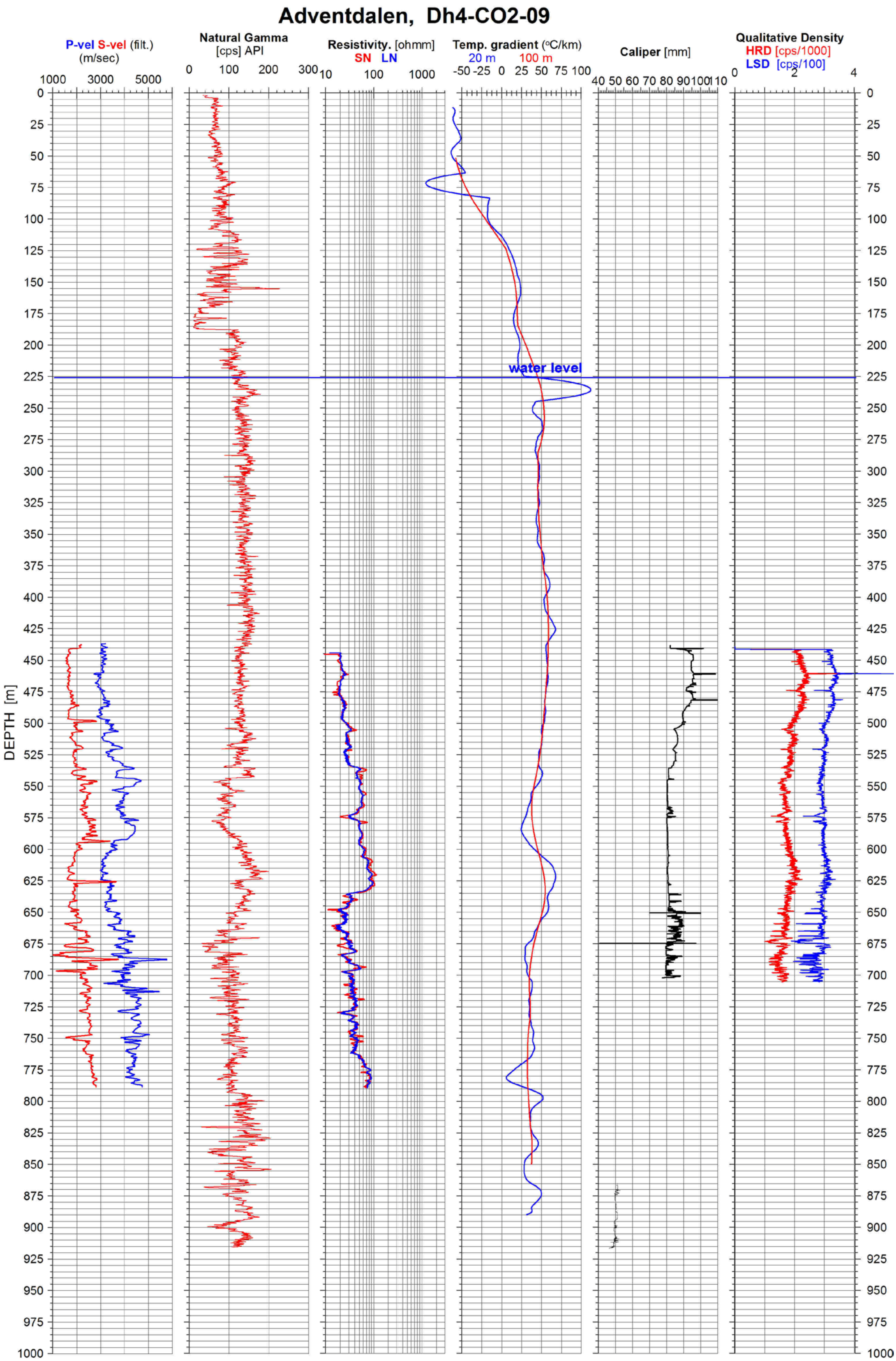

Figure 2. Dh4-CO2-09. P- and S-velocity, natural gamma, resistivity, thermal gradient, caliper, qualitative density

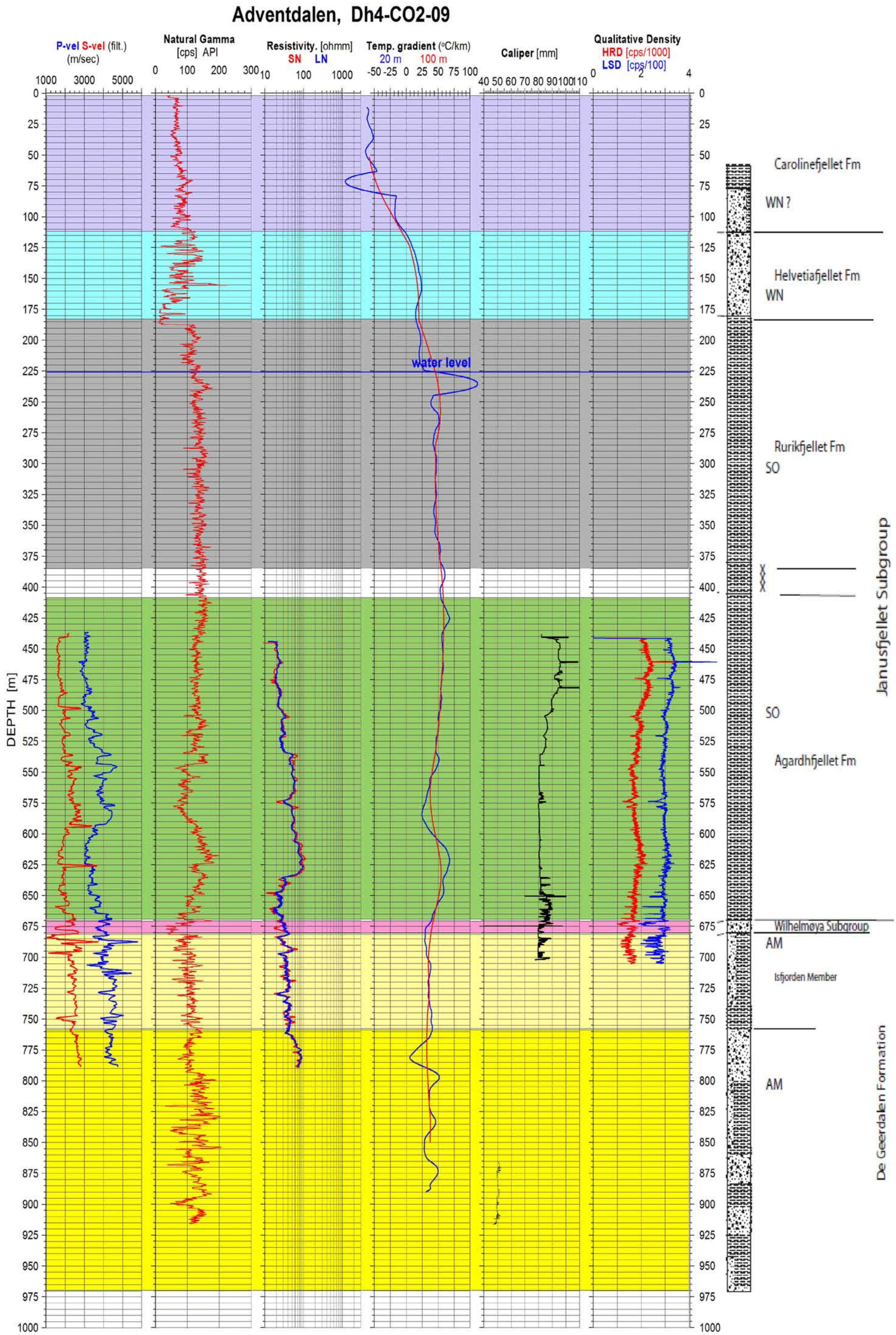

Figure 3. Dh4-CO2-09. P- and S-velocity, natural gamma, resistivity, thermal gradient, caliper, qualitative density. A stratigraphic log is shown to the right.

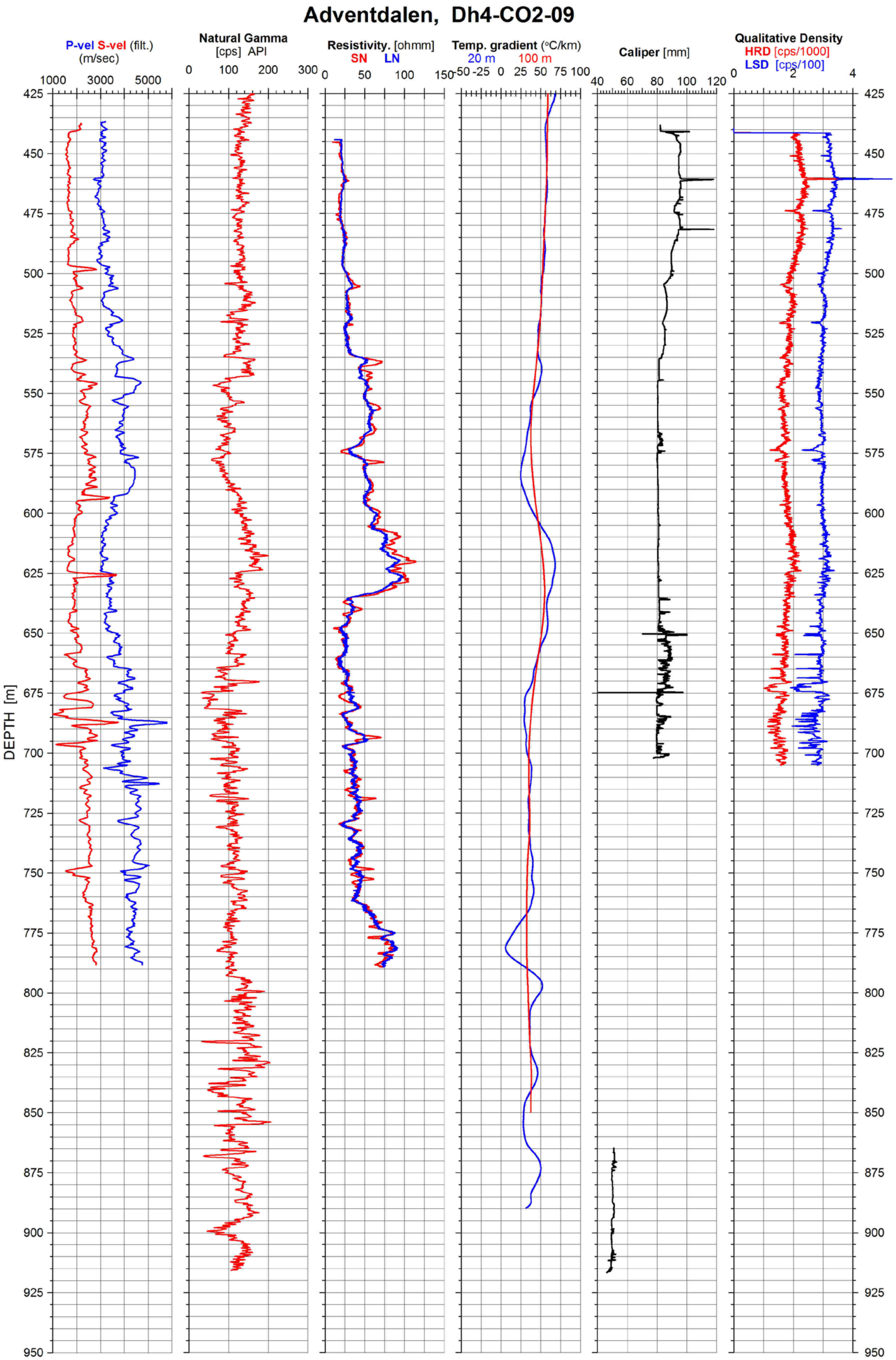

Figure 4. Dh4-CO_2-09. P- and S-velocity, natural gamma, resistivity, thermal gradient, caliper, qualitative density.

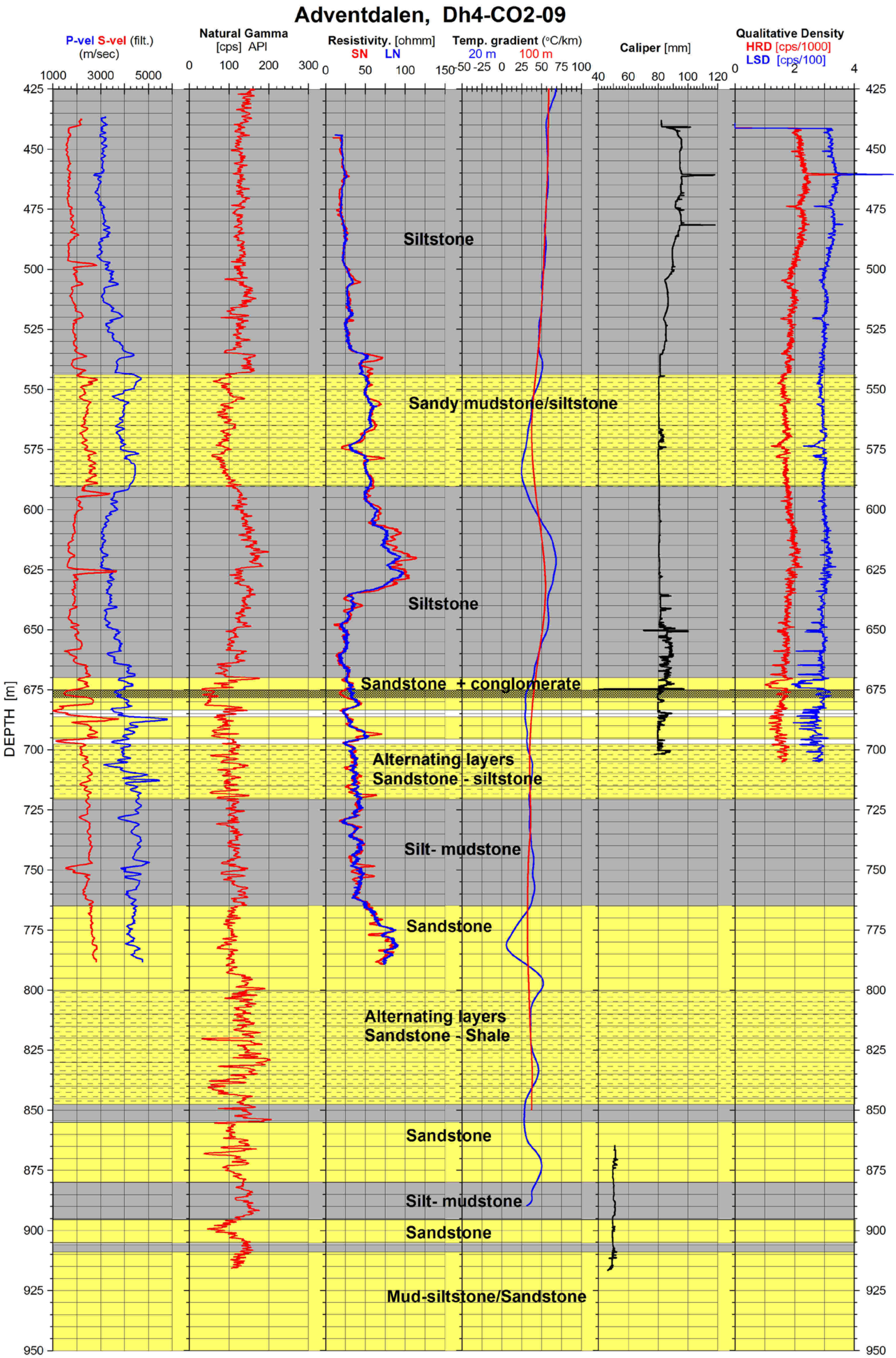

Figure 5. Dh4-CO_2-09. P- and S-velocity, natural gamma, resistivity, thermal gradient, caliper, qualitative density and simplified lithological interpretation log.

4.2 Acoustic televiewer

Acoustic televiewer was performed in Dh4 from 440 m to 705 m. The recorded image was of relatively poor quality because the probe was not well centralized in the borehole. This is so because the borehole diameter was too small for using the RG centralizer springs. However, the data could be interpreted with satisfying interpretation of fractures, and statistics of identified fractures have been worked out. Figure 6 shows an acoustic image of a section in Dh4, from 620 – 624 m depth. Most of the fractures in Dh4 are horizontal and parallel to the foliation. Detailed information about all fractures is listed in Appendix 1 and 2.

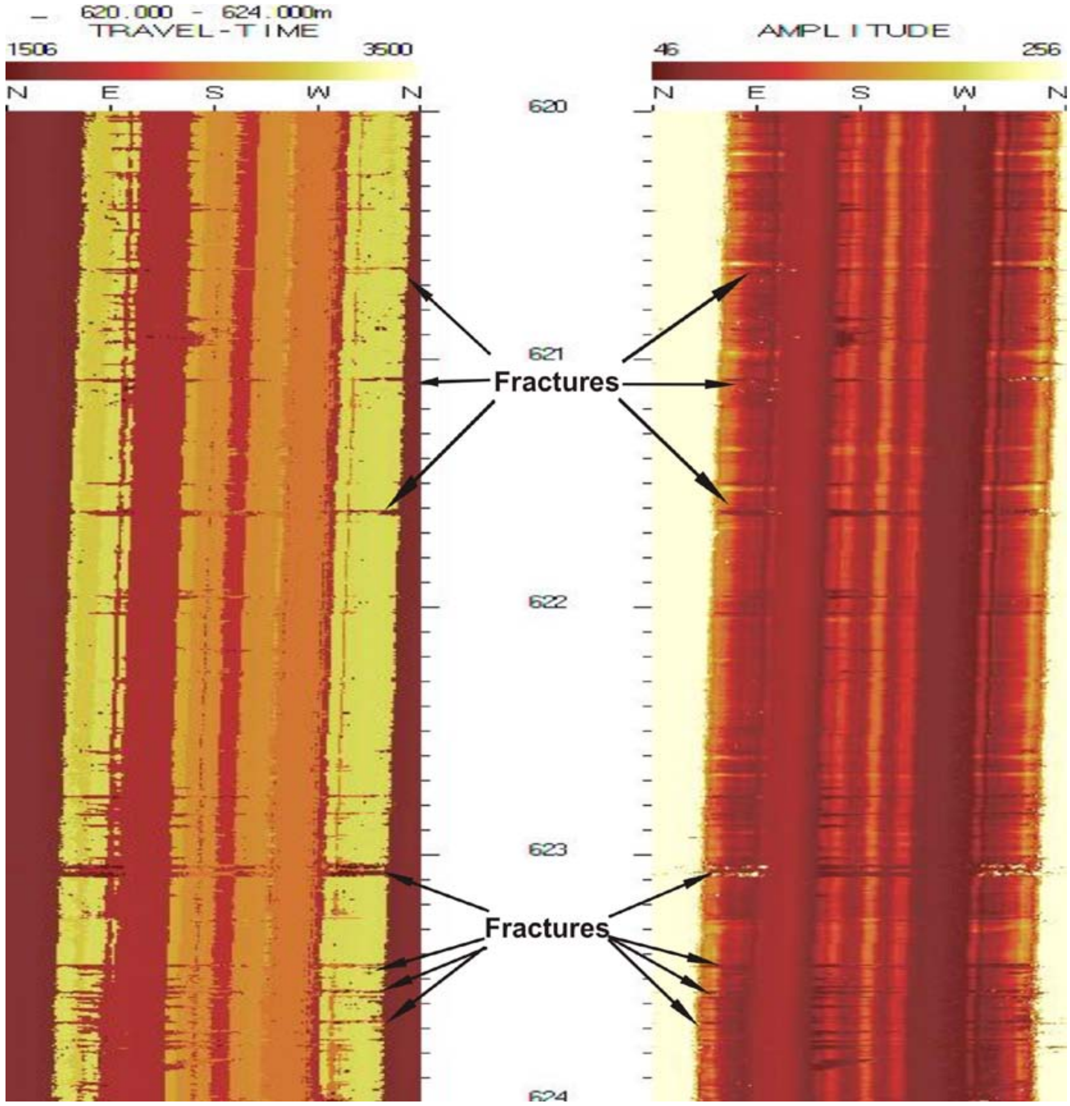

Figure 6. Acoustic image of section 620 – 624 m in Dh4 showing horizontal fractures. Travel-time image (left) and amplitude image (right).

4.2.1 Fracture stereogram

Figure 7 shows the fracture stereogram for all identified fractures in borehole Dh4-CO2. The blue group is the overall dominating set of fractures which basically is horizontal. Of 284 fractures, 258 belong to this set. There are three other sets with moderately dipping fractures, WNW - ESE and NE – SW striking. Mean strike and dip of all defined sets, as seen in the stereogram, are listed in the table in figure 7.

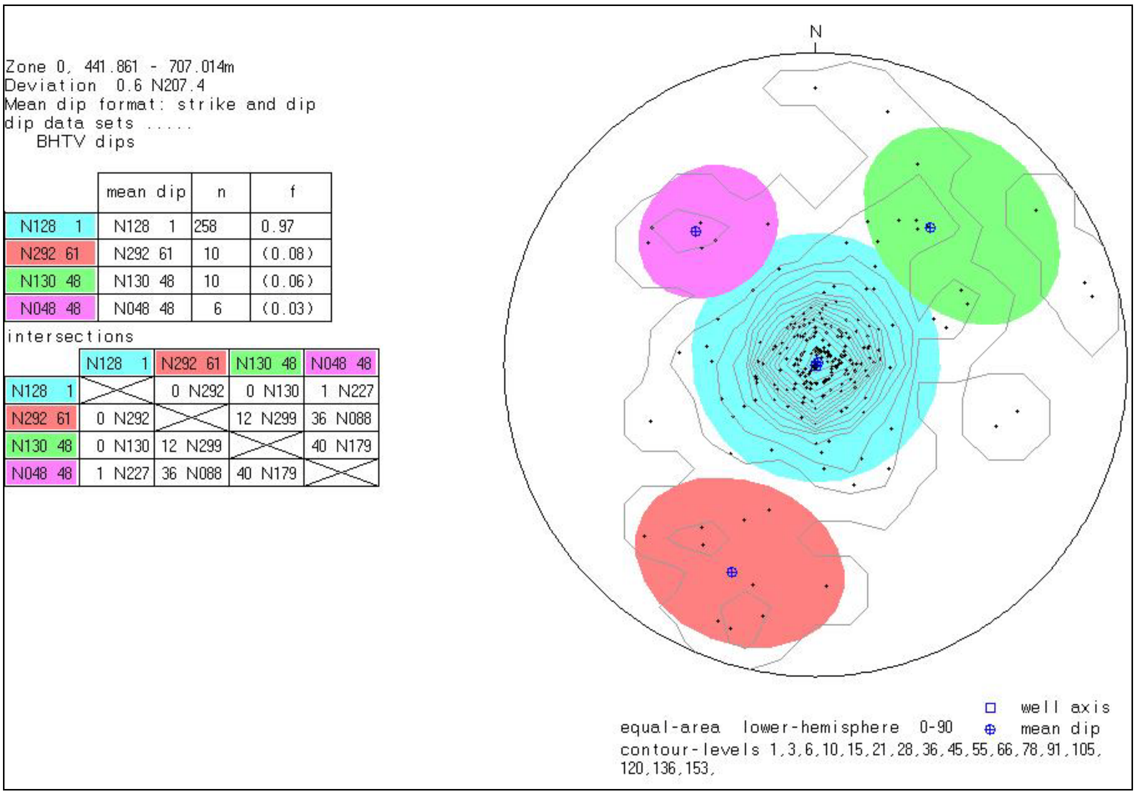

Figure 7. Fracture stereogram of indicated fractures in Dh4-CO2, showing contoured poles to surfaces (dots), and four identified fracture sets.

4.2.2 Fracture histograms

Different fracture sets are defined in the stereogram by different colors, see figure 7. The same sets and colors can be identified in the fracture histograms and on individual fractures.

Figure 8 shows the fracture frequency histograms for Dh4-CO_2, 440 m – 705 m. As seen in the stereogram, the blue group of fractures is dominating. It is obvious that the most fractured part of the borehole is 600 – 650 m. This is in the siltstone (590 – 670 m). Maximum fracture frequency is 6 fractures/meter. Other highly fractured sections in the borehole are: 455 – 475 m (siltstone), 498 – 504 m (siltstone), 535 – 545 m (siltstone), 658 – 664 m (siltstone) and 682 – 708 m (sandstone and siltstone). VJC (volume joint count) is the total fracture frequency from all fracture sets (colors).

Figure 9 shows seismic velocity, gamma, resistivity and caliper together with fracture frequency histograms for the horizontal fractures. Some of the fractured sections in the borehole fit well with lowered seismic velocity and lowered resistivity (yellow marking) while some does not. Especially this can be seen in the lower part of the logged borehole, below 650 m depth in the sandstone and alternating sandstone/siltstone. In the most fractured part, 600 – 650 m depth and in the upper part of the siltstone, the fractures do not seem to influence on the seismic velocity and resistivity in the same way. This could indicate that the fractures in the sandy layers are open and water filled. On the contrary this might also indicate that the fractured siltstone is tight.

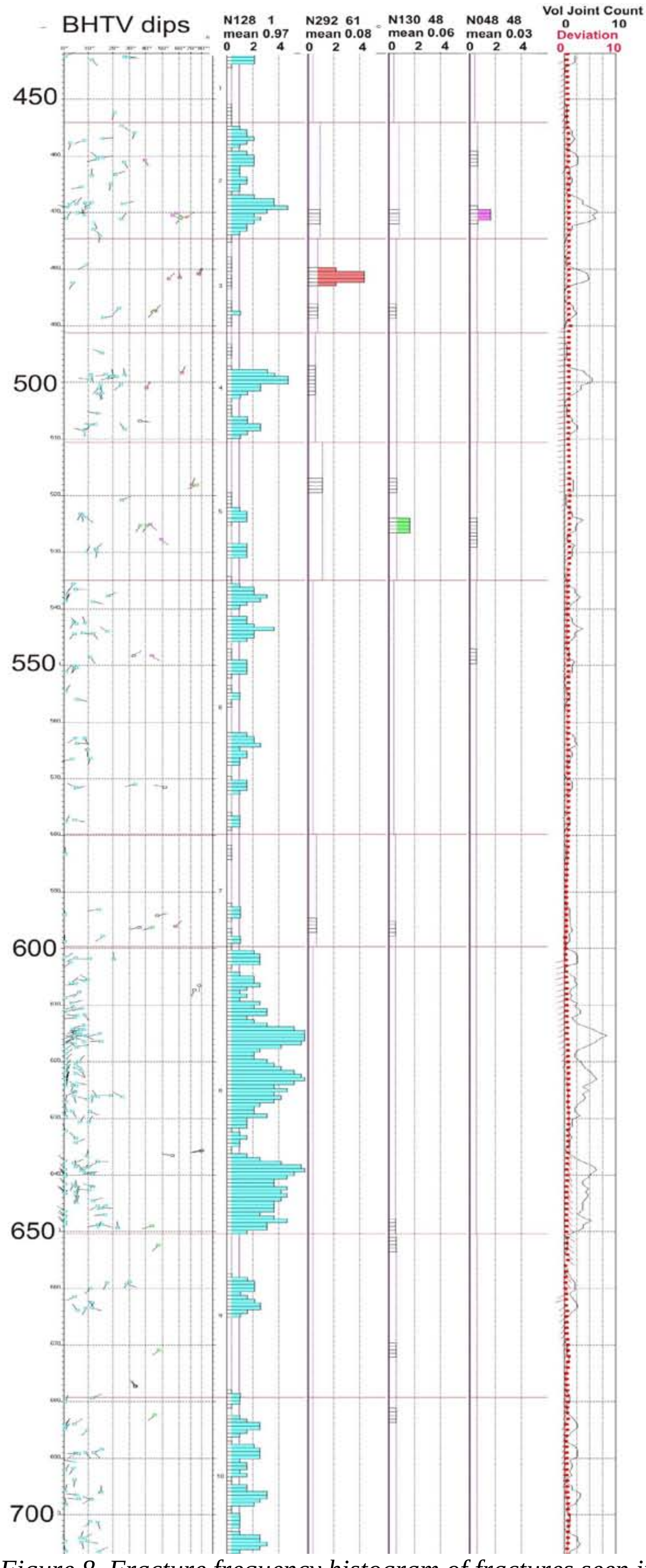

Figure 8. Fracture frequency histogram of fractures seen in televiewer in Dh4-CO_2. VJC (Volume Joint Count) is the total fracture frequency from all fracture sets.

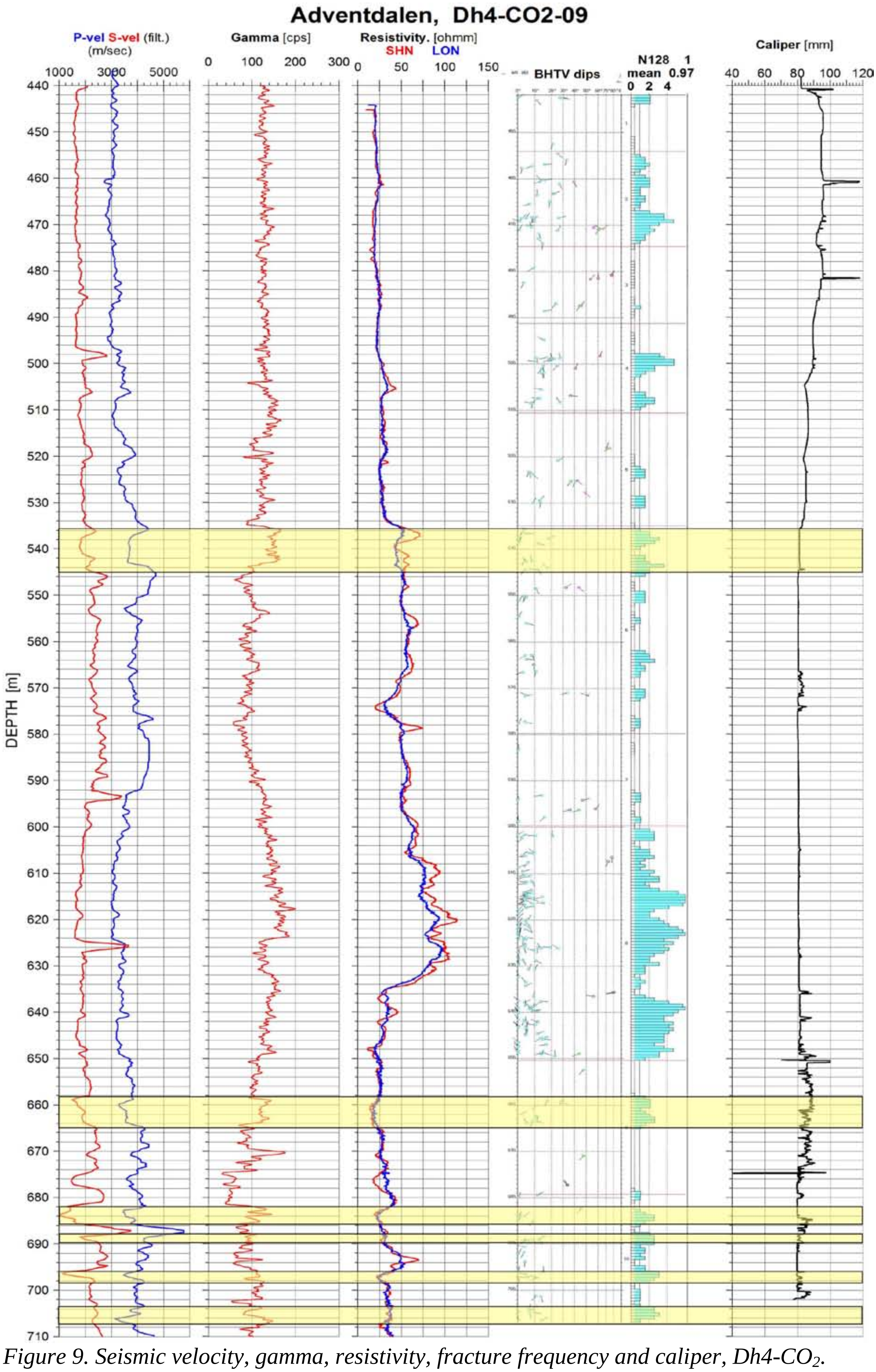

Figure 9. Seismic velocity, gamma, resistivity, fracture frequency and caliper, Dh4-CO_2.

4.3 Temperature and fluid conductivity.

Temperature and fluid conductivity were measured two times, 10.10.09 (790 m) and 02.12.09 (900 m). The water table was moved down 55 m from the first logging of 180 m to 235 m depth when the second logging took place. The results from both logs are shown in figure 10. The temperature at 900 m depth is 31.8 ^{o}C. The two temperature logs are quite similar below the water table, 0.7 ^{o}C higher on the first log which was done one day after ended drilling. The last log (02.12.09) was performed 5 days after ended drilling. Data from logging in air is inaccurate for this type of measurements. Note that the fluid conductivity is extremely high due to the use of salt in the drilling fluid.

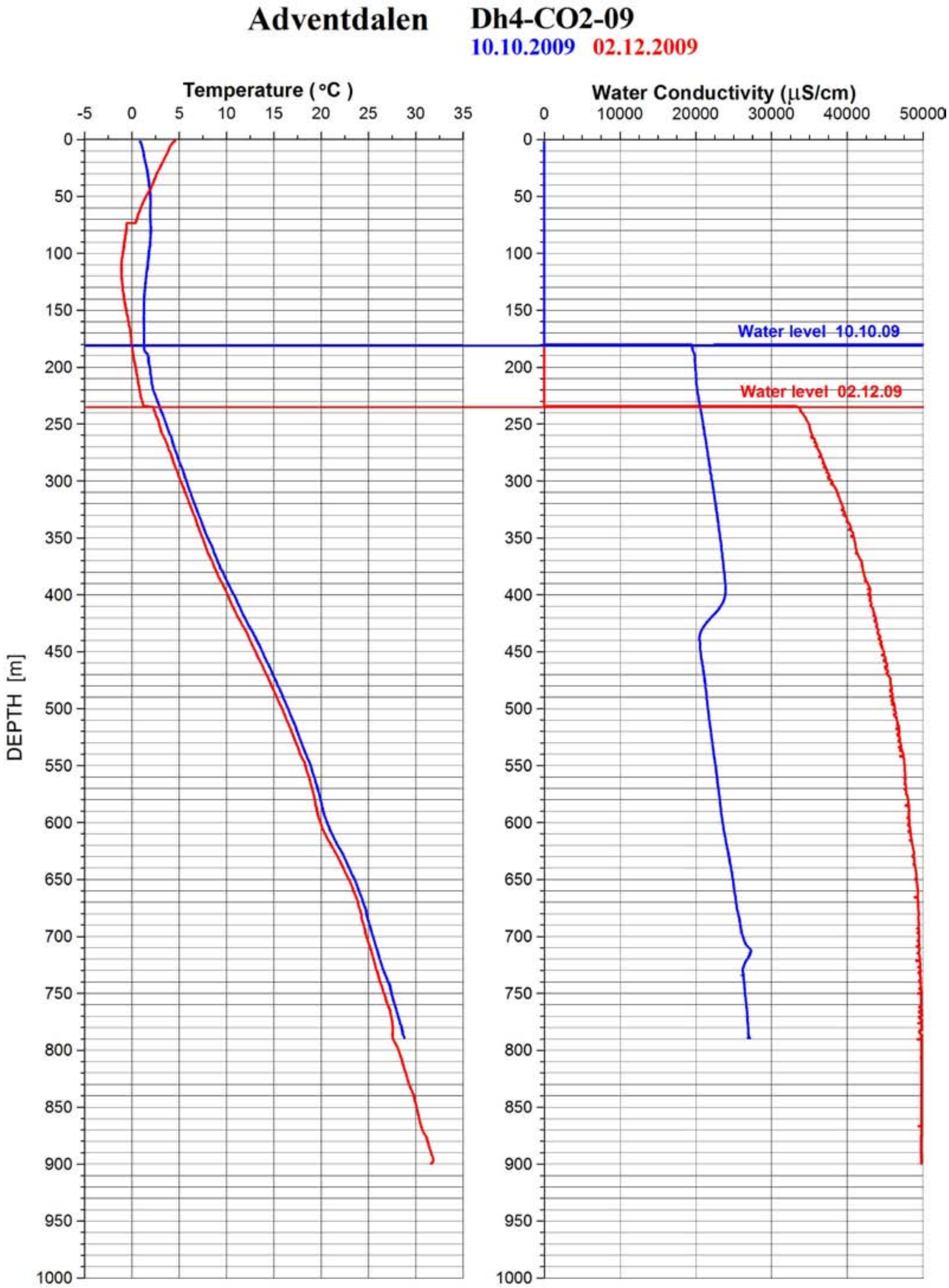

Figure10. Temperature and fluid conductivity in Dh4-CO_2-09. Blue lines are data from 10.10.09, the red lines from 02.12.09.

Temperature logging should be performed when the temperature in the well is stabilized after ended drilling. The time after drilling depends on drilling method, borehole diameter and drilling fluid temperature. Determination of temperature perturbation in oil wells after mud circulation can be done (Middelton 1982). Christophe Pascal, NGU, calculated the temperature perturbation in a 60 mm borehole 60 hours after mud circulation using a temperature difference of 10 - 40 ^{o}C between the drilling fluid temperature and the formation temperature. The results suggest that the formation temperature should not be much affected, 0.05 – 0.2 ^{o}C (Pascal personal information).

Figure 11 shows the thermal gradient in Dh4. The thermal gradients are calculated using running least-squares gradients of a straight line with depth intervals of 20 m and 100 m. The 20 m interval is more sensitive to local variations in the temperature. The thermal gradient is close to 50 ^{o}C/km in the mud- and siltstone down to 650 m depth. In the sandstone the gradient is lower, 35- 40 ^{o}C/km, due to the higher thermal conductivity in sandstone.

It is interesting to notice the decrease in thermal gradient at 545 – 590 m depth due to the increasing amount of sand in this section. In the underlying siltstone at 590 – 670 m, the thermal grading increases probably because of the lower thermal conductivity. The big decrease in the gradient at 760 – 785 m is caused by a layer of massive sandstone with higher thermal conductivity. Figure 12 shows the temperature, thermal gradient, gamma log and a simplified lithological log and clearly shows the correlation between the thermal gradient and the lithological units with different thermal conductivities. Also note the correlation to the gamma log.

Geothermal modeling shows that the thermal gradient is very sensitive to changes in the thermal conductivity (C. Pascal, pers. com.) and roughly the thermal conductivity in sandstone is twice the conductivity in mud-/siltstone. This could be confirmed by thermal conductivity measurements on cores from Dh 4. In general the thermal gradient at Svalbard is very high compared to thermal gradients measured onshore Norway, but is rather common for stable sedimentary basins.

Local changes in the temperature may also be caused by inflow of hot/cold water, but such changes are more abrupt than those seen in Dh4-CO_2. Inflow/outflow and vertical water flow can be measured with an impeller flowmeter. The borehole should not be cased.

Adventdalen Dh4-CO2-09

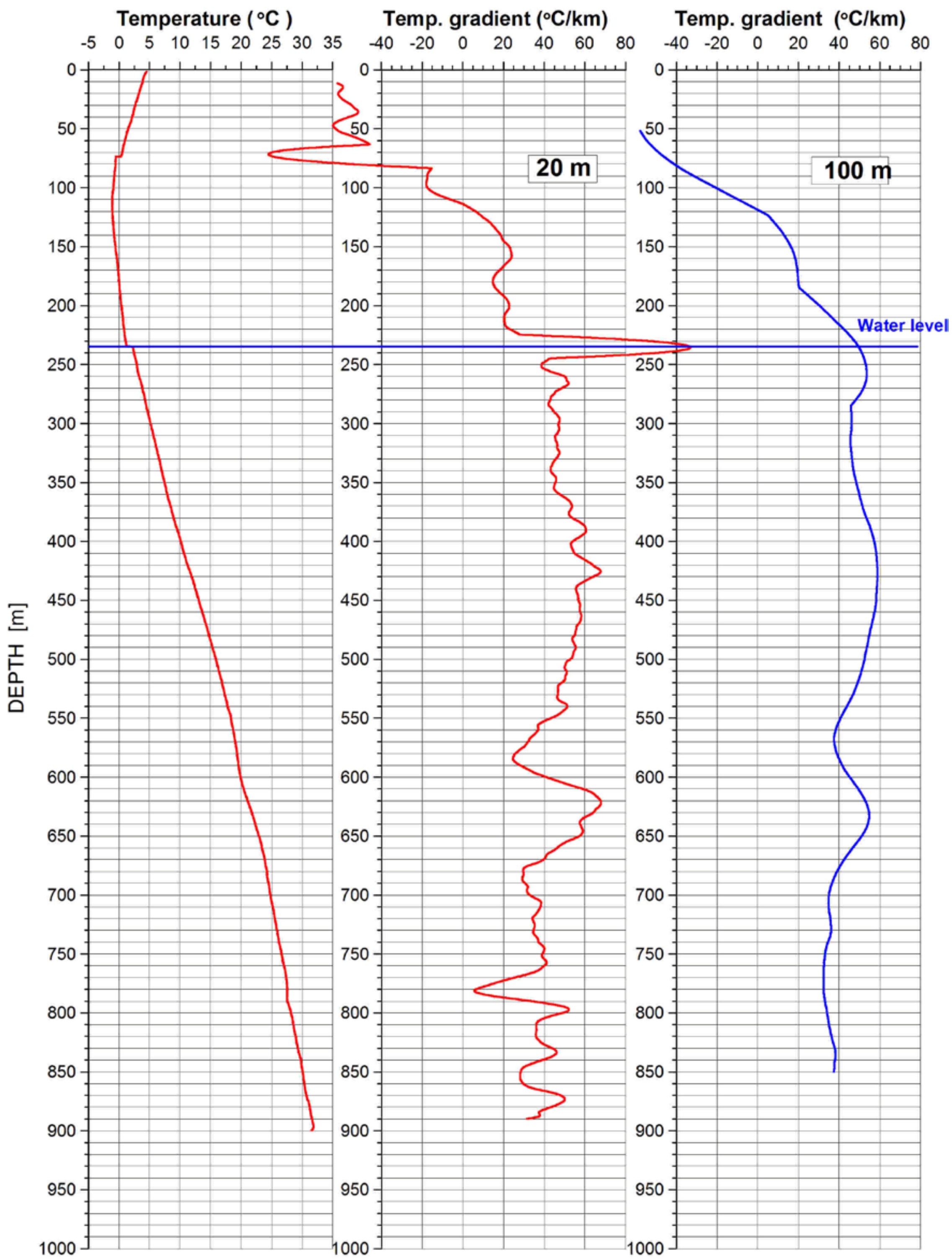

Figure 11. Temperature and thermal gradients in Dh4-CO_2-09 measured 02.12.09.

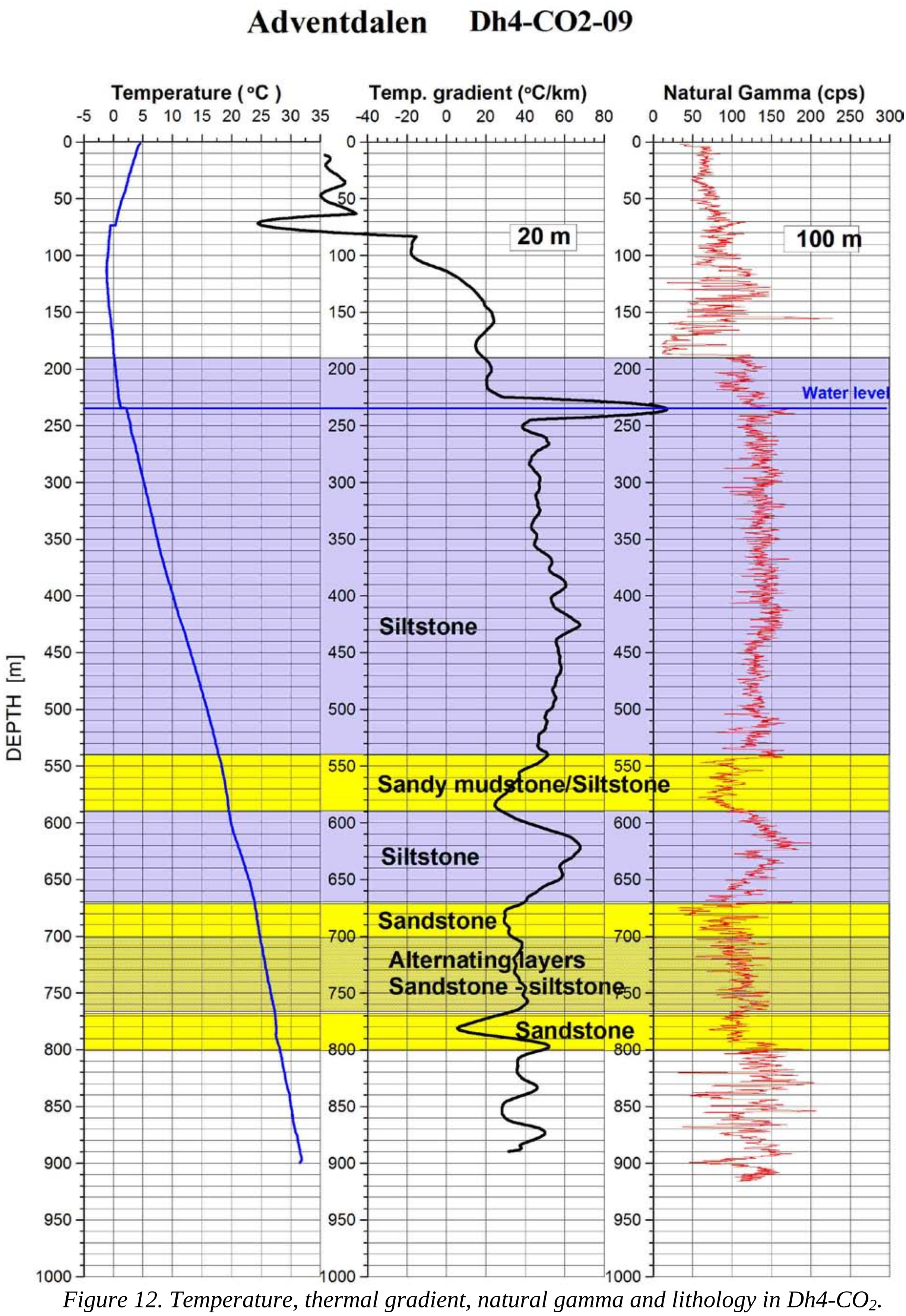

Figure 12. Temperature, thermal gradient, natural gamma and lithology in Dh4-CO_2.

4.4 Deviation

Deviation was measured from the surface to 712 m depth. Deviation components are shown in figure 13, confirming that the deviation from vertical is very small. At a depth of 712 m the East-component is 0.6 m and the North-component 3.6 m. The deviation from vertical of the borehole is towards the South. In the upper 440 m the azimuth is wrong due to the influence of magnetic material in the casing. Deviation data are listed in Appendix 3. Explanation of the data tables is given on the NGU web site.

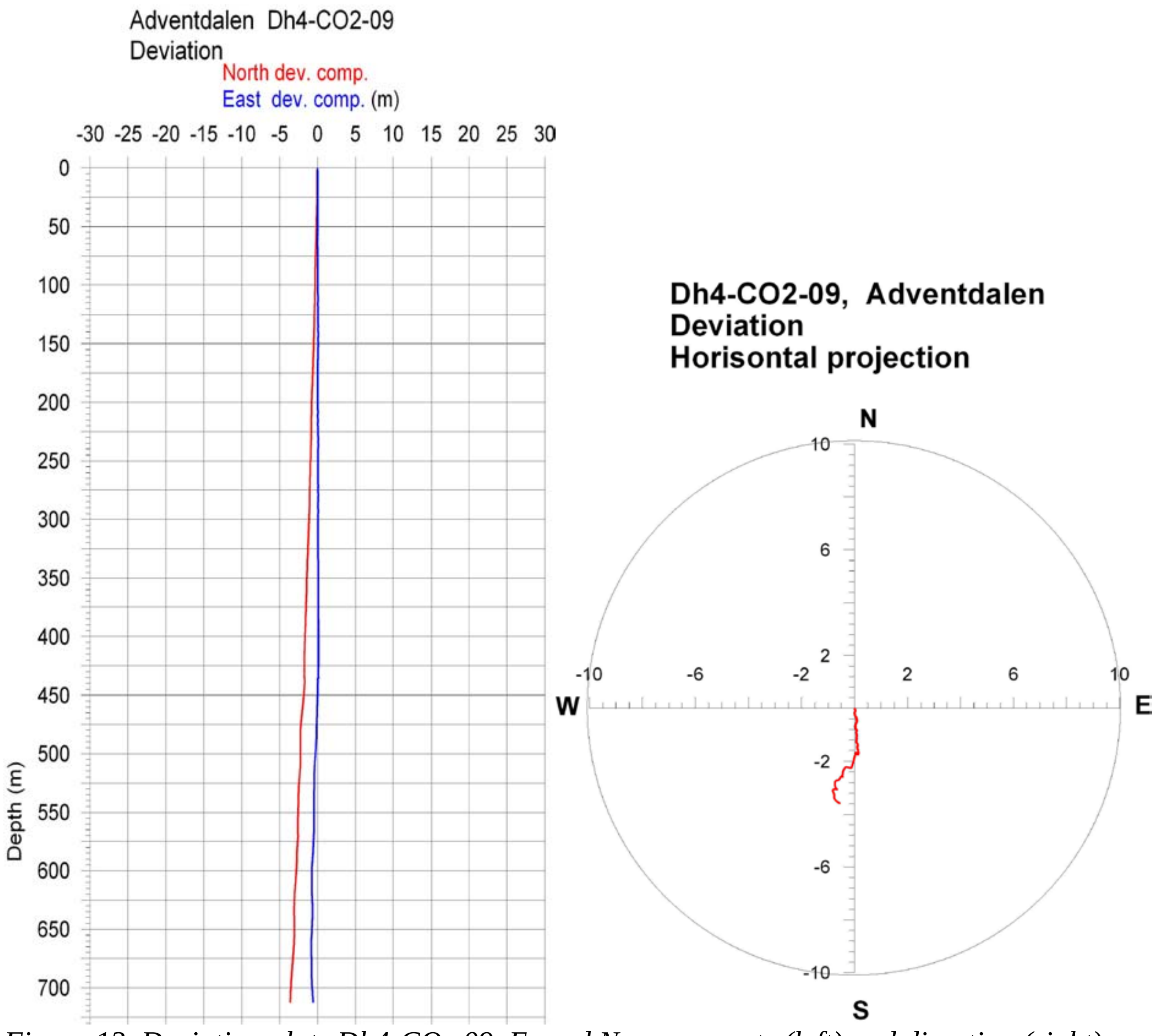

Figure 13. Deviation plots Dh4-CO_2-09, E- and N-components (left) and direction (right).

5. CONCLUTION

NGU has carried out borehole logging in the well LYB CO_2 Dh4, in Adventdalen 5 km outside Longyearbyen. The well was drilled to locate deep sandstone formations that may be used to store CO_2. UNIS and partners in the Longyearbyen CO_2 Lab project, will use the test site as laboratory for injection, storing and monitoring CO_2 in the underground. The well was drilled to 970 m and found injective Late Triassic sandstone.

Logging parameters were temperature, fluid conductivity, natural gamma, rock resistivity, seismic velocity, caliper, relative density and borehole deviation. The well was also inspected by acoustic televiewer to map fractures. Because of casing in the well and small borehole diameter in the deepest part, the entire borehole could not be logged.

The results show good correlation between the geophysical logs and the lithological units. Sandstones are indicated with low gamma radiation and increasing seismic velocity and apparent resistivity. Acoustic televiewer interpretation shows that some of the sandstones are highly fractured, which is confirmed by lowered seismic velocity and resistivity. Overlaying silt- and mudstones are more fractured but the fractures do not influence strongly on the seismic velocity and resistivity log.This indicates that the fractures in the sandy layers are open and water filled. This also indicates that the fractured siltstone is tight.

6. REFERENCES

Advanced Logic Technology, 2006: WellCAD, FWS processing, version 4.1.

Archie, G.E., 1942: The electrical resistivity log as an aid in determining some reservoir characteristics. *Petroleum Technology, 5, 1422 – 1430.*

Elvebakk, H. 2008: Results of borehole logging in CO_2 wells, Dh1-CO_2-07 and Dh2-CO_2-07, Longyearbyen, Svalbard. *NGU Report 2008.054.*

Middelton, M.F. 1982: Bottom hole temperature stabilization with continued circulation of drilling mud. *Geophysics, vol. 47. No 12. December 1982, p. 1716 – 1723.*

Schön, J.H. 2004: Physical Properities of Rocks, Fundamental and Principles of Petrophysics. *Volume 18, Elsevier.*

Thunhead, H. & Olsson, O. 2004: Borehole corrections for a thick resistivity probe. *JEEG, December 2004, Volume 9, Issue 4, pp. 217 – 224.*

	Depth	Azimuth	Dip	Upper Depth	Lower Depth	Well Diam	Well deviation Azimuth	Dev	Thickness
1	706.514	N050	14.3	706.504	706.524	0.08	171.73	0.58	0.0576
2	706.456	N350	0.7	706.456	706.456	0.08	170.5	0.66	0
3	704.865	N169	7.3	704.86	704.871	0.08	187.62	0.7	0
4	704.743	N107	9.7	704.736	704.75	0.08	165.2	0.78	0
5	704.661	N349	0.6	704.661	704.661	0.08	169.4	0.58	0
6	704.126	N043	8.6	704.12	704.131	0.08	173.89	0.66	0.0404
7	704.085	N014	6.6	704.081	704.089	0.08	197.87	0.55	0
8	701.326	N167	13.8	701.316	701.337	0.08	179.12	0.72	0.1051
9	701.219	N218	10.9	701.211	701.227	0.08	172.97	0.64	0
10	698.191	N357	0.7	698.191	698.191	0.08	177	0.7	0
11	697.325	N295	11.5	697.317	697.332	0.08	179.95	0.88	0
12	697.218	N231	11.2	697.21	697.226	0.08	190.37	0.71	0
13	697.174	N273	5.9	697.17	697.178	0.08	190.72	0.59	0
14	696.464	N275	5.2	696.46	696.467	0.08	184.34	0.7	0
15	696.081	N000	15.4	696.07	696.092	0.08	189	0.63	0
16	695.831	N008	0.6	695.831	695.831	0.08	188.2	0.6	0
17	693.749	N184	4.4	693.746	693.753	0.08	201	0.51	0
18	692.17	N022	0.5	692.17	692.17	0.08	202	0.46	0
19	691.778	N202	3.8	691.775	691.781	0.08	201	0.45	0
20	690.633	N285	4.3	690.629	690.636	0.08	210.51	0.43	0
21	689.161	N268	6	689.157	689.166	0.08	206.68	0.48	0
22	689.089	N222	4.9	689.085	689.092	0.08	206.89	0.41	0
23	689.044	N149	8.9	689.037	689.05	0.08	204	0.46	0.0359
24	689.007	N148	12.6	688.998	689.016	0.08	206.2	0.46	0
25	688.412	N241	15.5	688.401	688.423	0.08	203	0.46	0
26	685.112	N218	9.7	685.105	685.119	0.08	204.32	0.52	0
27	684.945	N025	0.5	684.945	684.945	0.08	205	0.52	0
28	684.365	N018	0.5	684.365	684.365	0.08	198	0.51	0
29	684.015	N027	0.6	684.015	684.015	0.08	207	0.55	0
30	683.957	N042	4.3	683.955	683.96	0.08	200	0.53	0
31	682.359	N217	45.4	682.317	682.4	0.08	200.35	0.58	0
32	679.985	N017	0.6	679.985	679.985	0.08	197	0.59	0
33	679.367	N057	11.6	679.359	679.375	0.08	197	0.59	0
34	677.336	N342	33.5	677.31	677.362	0.08	193	0.64	0.0734
35	677.248	N325	33.7	677.222	677.274	0.08	197.72	0.59	0
36	670.892	N219	47.7	670.847	670.937	0.08	200.09	0.68	0
37	663.837	N334	5.4	663.834	663.841	0.08	218.26	0.39	0
38	663.534	N199	8.9	663.527	663.54	0.08	209	0.45	0
39	663.492	N114	11.6	663.484	663.501	0.08	222	0.5	0
40	662.567	N178	11.7	662.559	662.576	0.08	242.04	0.34	0
41	662.522	N164	10.9	662.515	662.53	0.08	248	0.32	0
42	661.522	N235	4.3	661.519	661.525	0.08	230.28	0.38	0
43	659.993	N215	11	659.985	660.001	0.08	166.79	0.26	0.6721
44	659.299	N115	28.4	659.277	659.321	0.08	152.77	0.29	0
45	659.042	N198	17.6	659.029	659.055	0.08	149.54	0.26	0
46	658.913	N211	30.3	658.889	658.936	0.08	148.73	0.27	0
47	652.391	N215	47.3	652.348	652.435	0.08	146.93	0.4	0
48	649.351	N356	23.2	649.334	649.368	0.08	128.61	0.46	0.1081
49	649.237	N015	14.2	649.227	649.247	0.08	139.21	0.41	0
50	648.901	N243	43.7	648.863	648.939	0.08	143	0.45	0
51	648.824	N253	14.2	648.814	648.834	0.08	145.6	0.47	0
52	648.73	N112	15.6	648.718	648.741	0.08	141.52	0.45	0
53	648.65	N326	0.5	648.65	648.65	0.08	145.5	0.47	0
54	648.29	N324	0.4	648.29	648.29	0.08	144	0.42	0
55	647.45	N317	0.4	647.45	647.45	0.08	137.5	0.4	0
56	647.22	N325	0.4	647.22	647.22	0.08	145.5	0.42	0
57	646.986	N265	17	646.974	646.998	0.08	144.9	0.37	0
58	646.47	N319	0.5	646.47	646.47	0.08	139.49	0.47	0
59	645.774	N094	15.2	645.763	645.785	0.08	148.79	0.42	0
60	645.469	N230	13.8	645.459	645.479	0.08	145.2	0.43	0
61	645.376	N234	17.1	645.364	645.389	0.08	146	0.43	0
62	644.848	N013	5.1	644.845	644.852	0.08	146.32	0.46	0
63	644.758	N002	4.8	644.755	644.761	0.08	146	0.46	0
64	644.532	N064	12.1	644.523	644.54	0.08	144	0.45	0
65	643.638	N013	5.1	643.635	643.641	0.08	148	0.47	0
66	643.205	N331	0.5	643.205	643.205	0.08	151.01	0.49	0
67	643.043	N019	4.8	643.04	643.046	0.08	149.81	0.53	0
68	642.905	N318	0.5	642.905	642.905	0.08	138	0.53	0
69	642.875	N319	0.5	642.875	642.875	0.08	139	0.5	0
70	642.656	N278	10.6	642.649	642.663	0.08	145.92	0.48	0

71	642.118	N300	12	642.11	642.126	0.08	141.47	0.61	0
72	642.067	N358	5.1	642.064	642.071	0.08	144	0.52	0
73	641.612	N196	3.9	641.609	641.615	0.08	146.1	0.41	0
74	641.56	N331	0.4	641.56	641.56	0.08	150.5	0.45	0
75	640.16	N334	0.5	640.16	640.16	0.08	154	0.51	0
76	639.96	N332	0.5	639.96	639.96	0.08	152	0.5	0
77	639.775	N331	0.5	639.775	639.775	0.08	151	0.5	0.0614
78	639.713	N268	11.9	639.705	639.722	0.08	153	0.49	0
79	639.625	N081	9.2	639.619	639.632	0.08	150.98	0.51	0
80	639.289	N048	7.3	639.284	639.294	0.08	150.44	0.53	0
81	639.225	N331	7.8	639.22	639.23	0.08	152	0.54	0
82	639.01	N332	0.5	639.01	639.01	0.08	152	0.5	0
83	638.86	N047	7.2	638.855	638.865	0.08	153.54	0.5	0
84	638.512	N357	4.7	638.509	638.515	0.08	151.71	0.52	0
85	638.478	N049	10.2	638.471	638.485	0.08	152	0.53	0
86	637.858	N059	4	637.855	637.861	0.08	151.31	0.5	0
87	637.568	N092	13.9	637.557	637.578	0.08	145	0.54	0
88	637.515	N324	0.5	637.515	637.515	0.08	144.01	0.54	0
89	636.584	N007	9.6	636.577	636.59	0.08	154.55	0.58	0
90	636.545	N283	56.1	636.486	636.604	0.08	162	0.57	0
91	635.712	N253	79.2	635.503	635.922	0.08	158	0.63	0.0172
92	635.614	N256	80.6	635.373	635.855	0.08	158.92	0.63	0
93	634.233	N057	4.8	634.23	634.236	0.08	156.29	0.62	0
94	633.513	N326	4.8	633.51	633.516	0.08	165	0.72	0
95	632.21	N346	0.7	632.21	632.21	0.08	166	0.72	0
96	630.693	N020	10.4	630.686	630.7	0.08	169	0.77	0
97	630.666	N022	6.6	630.662	630.67	0.08	169	0.77	0
98	629.69	N353	0.8	629.69	629.69	0.08	173	0.76	0
99	628.788	N123	10.7	628.78	628.796	0.08	176.27	0.75	0
100	628.672	N160	3.2	628.669	628.675	0.08	174	0.76	0.0972
101	628.575	N356	0.8	628.575	628.575	0.08	176	0.79	0
102	627.09	N002	0.8	627.09	627.09	0.08	182.01	0.76	0
103	626.649	N292	9.7	626.642	626.655	0.08	178.64	0.72	0
104	626.203	N310	26.1	626.184	626.222	0.08	184.19	0.75	0.0865
105	626.111	N331	13.9	626.102	626.121	0.08	184	0.75	0
106	625.987	N187	12	625.978	625.996	0.08	185	0.74	0
107	625.957	N172	4	625.953	625.96	0.08	184.83	0.75	0
108	625.904	N272	19.5	625.89	625.918	0.08	185	0.75	0
109	625.304	N240	4.5	625.3	625.307	0.08	186.15	0.75	0
110	624.31	N009	0.8	624.31	624.31	0.08	189	0.78	0
111	624.257	N318	5.1	624.253	624.26	0.08	191.83	0.75	0
112	624.182	N188	3.6	624.179	624.185	0.08	190.31	0.76	0
113	623.673	N105	4.9	623.67	623.677	0.08	190.36	0.79	0
114	623.55	N013	0.8	623.55	623.55	0.08	193	0.78	0
115	623.45	N014	0.8	623.45	623.45	0.08	194	0.76	0
116	623.08	N016	0.8	623.08	623.08	0.08	196	0.76	0
117	623.05	N016	0.8	623.05	623.05	0.08	196	0.77	0
118	622.835	N018	0.8	622.835	622.835	0.08	198	0.78	0
119	622.76	N017	0.8	622.76	622.76	0.08	197	0.76	0
120	622.028	N126	4.8	622.025	622.032	0.08	200.34	0.75	0
121	621.96	N020	0.7	621.96	621.96	0.08	200	0.74	0
122	621.615	N159	7.1	621.61	621.62	0.08	201	0.74	0
123	621.505	N024	0.8	621.505	621.505	0.08	204	0.75	0
124	621.078	N126	4.6	621.075	621.082	0.08	205	0.74	0
125	620.635	N027	0.7	620.635	620.635	0.08	207	0.72	0
126	620.393	N141	4.7	620.39	620.397	0.08	207	0.71	0
127	619.938	N031	6	619.934	619.942	0.08	209	0.7	0
128	619.505	N032	0.7	619.505	619.505	0.08	212	0.71	0
129	618.65	N037	0.7	618.65	618.65	0.08	217	0.71	0
130	617.78	N041	0.7	617.78	617.78	0.08	220.5	0.72	0
131	617.458	N326	5	617.455	617.462	0.08	224	0.7	0
132	617.098	N262	9.2	617.092	617.105	0.08	229	0.64	0
133	616.702	N275	4.2	616.699	616.705	0.08	231.28	0.59	0
134	616.66	N051	0.6	616.66	616.66	0.08	231.5	0.58	0
135	616.58	N051	0.6	616.58	616.58	0.08	231.5	0.58	0
136	616.425	N306	8.4	616.419	616.431	0.08	231.03	0.58	0
137	616.311	N267	15.3	616.299	616.322	0.08	232.43	0.55	0
138	615.867	N296	4.6	615.863	615.87	0.08	232	0.53	0
139	615.506	N121	8.7	615.5	615.512	0.08	230.9	0.52	0
140	615.428	N220	4.1	615.425	615.431	0.08	231	0.51	0
141	615.33	N268	9.7	615.322	615.337	0.08	231.64	0.5	0
142	615.214	N240	4.6	615.21	615.217	0.08	231	0.5	0
143	615.119	N257	6.4	615.114	615.124	0.08	231	0.5	0
144	615.049	N251	14.7	615.038	615.06	0.08	232.57	0.51	0
145	614.639	N253	5.5	614.635	614.643	0.08	231	0.51	0
146	614.348	N264	6.8	614.343	614.353	0.08	231	0.52	0
147	614.323	N248	7.2	614.318	614.329	0.08	232.69	0.51	0
148	614.271	N280	8.3	614.265	614.277	0.08	231.62	0.5	0

149	614.207	N176	3.6	614.205	614.21	0.08	233.32	0.51	0
150	613.514	N251	8.3	613.508	613.52	0.08	232	0.51	0
151	612.163	N259	4.6	612.16	612.167	0.08	235.48	0.5	0
152	611.814	N277	5.4	611.81	611.818	0.08	234.13	0.5	0
153	611.622	N152	8.5	611.616	611.628	0.08	233.34	0.48	0
154	610.8	N055	0.5	610.8	610.8	0.08	235.5	0.46	0
155	610.602	N235	4	610.599	610.605	0.08	235.68	0.44	0.044
156	610.558	N251	7.4	610.552	610.563	0.08	235.74	0.45	0
157	609.542	N069	3.1	609.54	609.544	0.08	237	0.44	0
158	608.63	N062	0.4	608.63	608.63	0.08	242	0.44	0
159	607.601	N213	6.3	607.596	607.606	0.08	243	0.43	0
160	607.338	N196	73.5	607.2	607.476	0.08	242.69	0.42	0
161	606.524	N180	77.8	606.336	606.713	0.08	243.05	0.41	0
162	606.223	N260	4.7	606.219	606.226	0.08	244.86	0.39	0
163	606.121	N036	2.9	606.119	606.123	0.08	246	0.41	0
164	605.711	N286	8.6	605.705	605.717	0.08	247.4	0.39	0
165	605.523	N316	9.8	605.516	605.53	0.08	247.42	0.38	0
166	602.474	N223	2.6	602.472	602.476	0.08	249	0.36	0
167	601.856	N359	20.8	601.841	601.871	0.08	245.92	0.35	0
168	601.788	N269	10.6	601.78	601.796	0.08	248	0.35	0
169	601.582	N238	4.7	601.579	601.586	0.08	249.87	0.16	0
170	601.555	N053	0.3	601.555	601.555	0.08	233	0.25	0
171	598.72	N001	0.3	598.72	598.72	0.08	180.99	0.28	0
172	597.821	N223	16.1	597.81	597.833	0.08	181.27	0.28	0
173	596.288	N248	43.8	596.25	596.327	0.08	178.77	0.28	0.0477
174	596.226	N254	36	596.197	596.255	0.08	180	0.29	0
175	596.059	N032	57.7	595.996	596.122	0.08	178.6	0.29	0
176	594.185	N071	46.7	594.142	594.227	0.08	179.95	0.33	0
177	593.96	N358	0.3	593.96	593.96	0.08	178.5	0.31	0
178	593.149	N262	14.3	593.139	593.159	0.08	178.59	0.31	0
179	583.305	N001	0.5	583.305	583.305	0.08	181	0.54	0
180	577.645	N020	0.8	577.645	577.645	0.08	200	0.76	0
181	577.268	N106	4.4	577.265	577.271	0.08	200.3	0.75	0
182	571.677	N069	4.9	571.674	571.68	0.08	197.69	0.78	0
183	571.482	N303	5	571.478	571.485	0.08	197	0.79	0
184	571.48	N289	51.3	571.43	571.53	0.08	197	0.79	0
185	570.952	N249	33.5	570.925	570.979	0.08	202.68	0.82	0
186	566.524	N251	3.4	566.521	566.526	0.08	197	0.77	0
187	566.358	N193	10.9	566.35	566.366	0.08	195.29	0.77	0
188	564.91	N180	9.7	564.902	564.917	0.08	195	0.75	0
189	563.76	N093	5.2	563.756	563.763	0.08	194.46	0.75	0
190	562.875	N228	4.6	562.871	562.878	0.08	195.04	0.73	0
191	562.85	N155	8.3	562.844	562.856	0.08	194.51	0.74	0
192	562.824	N162	8.7	562.818	562.831	0.08	195	0.74	0
193	555.98	N107	5.3	555.976	555.983	0.08	199	0.79	0
194	554.516	N023	0.8	554.516	554.516	0.08	203	0.79	0
195	551.111	N029	0.8	551.111	551.111	0.08	209.4	0.83	0
196	550.37	N208	5	550.366	550.374	0.08	210.51	0.83	0
197	550.133	N189	4.1	550.129	550.136	0.08	208.77	0.81	0
198	548.463	N157	11.1	548.455	548.471	0.08	206.22	0.78	0
199	548.306	N136	43.5	548.268	548.345	0.08	205	0.77	0
200	548.301	N044	32.6	548.276	548.325	0.08	205	0.77	0
201	544.349	N211	4.3	544.346	544.353	0.08	195.42	0.66	0
202	544.283	N153	11.9	544.274	544.292	0.08	195.2	0.65	0
203	544.236	N103	7.7	544.231	544.242	0.08	195	0.66	0
204	543.955	N314	17.8	543.942	543.967	0.08	196.96	0.67	0
205	542.579	N334	5	542.576	542.582	0.08	196.42	0.65	0
206	542.531	N347	8.6	542.525	542.537	0.08	195	0.65	0
207	542.274	N200	4.1	542.271	542.278	0.08	194.07	0.65	0
208	538.708	N111	12	538.699	538.716	0.08	197.75	0.68	0
209	538.546	N018	0.7	538.546	538.546	0.08	197.8	0.68	0
210	538.341	N018	0.7	538.341	538.341	0.08	198	0.67	0
211	537.66	N059	18.3	537.647	537.673	0.08	198.5	0.69	0
212	537.606	N019	0.7	537.606	537.606	0.08	199	0.69	0
213	536.534	N091	4.7	536.531	536.537	0.08	202.91	0.74	0
214	535.599	N202	3.9	535.596	535.602	0.08	195.42	0.67	0
215	529.992	N020	9.3	529.986	529.998	0.08	212.32	1	0
216	529.757	N185	13.7	529.747	529.768	0.08	212	1.01	0
217	529.438	N034	13.1	529.43	529.447	0.08	212.32	1	0
218	527.718	N141	49.1	527.671	527.765	0.08	216.3	1.01	0
219	525.306	N200	40.6	525.27	525.341	0.08	222	1.06	0
220	525.247	N207	36.6	525.216	525.278	0.08	221.38	1.04	0
221	525.136	N141	42.6	525.099	525.173	0.08	218.15	1.02	0
222	523.863	N142	9.4	523.856	523.87	0.08	221.44	1.06	0
223	523.376	N177	7.4	523.37	523.381	0.08	224.06	0.98	0.1042
224	523.271	N196	6.8	523.265	523.276	0.08	224	1.06	0
225	520.794	N058	25.7	520.776	520.813	0.08	229	1.04	0
226	518.144	N235	75.5	517.978	518.276	0.08	253.86	0.95	0

227	518.08	N012	71.1	517.966	518.194	0.08	253	0.96	0
228	508.501	N288	8.3	508.495	508.508	0.08	260.62	0.83	0
229	508.3	N183	8.6	508.294	508.306	0.08	260	0.84	0
230	508.257	N334	27.4	508.236	508.278	0.08	261	0.84	0
231	507.493	N203	10.9	507.485	507.501	0.08	258	0.84	0
232	507.425	N277	13	507.415	507.435	0.08	259	0.82	0
233	506.838	N095	36.4	506.81	506.867	0.08	262	0.83	0
234	505.447	N283	14	505.437	505.458	0.08	256	0.83	0
235	501.919	N155	14.1	501.909	501.929	0.08	264	0.92	0
236	501.834	N190	15.9	501.823	501.846	0.08	264	0.94	0
237	500.986	N214	14.3	500.975	500.996	0.08	263.08	0.93	0
238	500.958	N018	40.5	500.924	500.991	0.08	263.25	0.94	0
239	500.431	N175	15.1	500.42	500.441	0.08	264.56	0.94	0
240	500.344	N218	25.2	500.324	500.363	0.08	264	0.93	0
241	499.429	N279	10.6	499.421	499.437	0.08	262.38	0.97	0
242	499.022	N240	19.2	499.008	499.037	0.08	262.26	0.94	0.1122
243	498.902	N243	22.7	498.885	498.92	0.08	259.56	0.93	0
244	498.807	N350	20.4	498.792	498.822	0.08	258.64	0.86	0.0652
245	498.735	N355	27.3	498.715	498.756	0.08	262.96	0.95	0
246	498.649	N171	11.3	498.641	498.657	0.08	263	0.95	0.0496
247	498.599	N257	17.1	498.585	498.612	0.08	264	0.95	0
248	498.309	N016	62.5	498.234	498.385	0.08	264	0.94	0
249	494.79	N304	15.6	494.779	494.802	0.08	264	0.91	0
250	488.567	N073	16.2	488.556	488.579	0.08	209	0.91	0
251	487.454	N210	44.7	487.413	487.495	0.08	208.84	0.91	0
252	487.414	N025	45.7	487.374	487.453	0.08	208.87	0.93	0
253	486.958	N214	23.9	486.939	486.976	0.08	208	0.92	0
254	482.463	N198	3.6	482.46	482.466	0.08	206.81	0.89	0
255	481.686	N035	53.6	481.633	481.738	0.08	206	0.88	0.124
256	481.467	N357	60.2	481.399	481.535	0.08	206.22	0.89	0
257	480.921	N018	78.1	480.745	481.097	0.08	205.4	0.89	0.0237
258	480.811	N021	77.1	480.647	480.974	0.08	206	0.9	0
259	479.306	N238	9.3	479.299	479.313	0.08	205.14	0.89	0
260	474.09	N187	14.8	474.079	474.101	0.08	202.97	0.88	0
261	472.915	N143	12.3	472.906	472.924	0.08	204	0.86	0
262	471.72	N165	12.4	471.71	471.729	0.08	204	0.87	0
263	471.147	N027	25.2	471.129	471.165	0.08	205	0.86	0
264	471.051	N023	0.8	471.051	471.051	0.08	203	0.85	0
265	470.888	N207	61.3	470.812	470.963	0.08	203	0.84	0
266	470.753	N045	66.7	470.663	470.782	0.08	203.77	0.85	0
267	470.528	N126	56.2	470.468	470.588	0.08	203.66	0.86	0
268	470.386	N343	8.3	470.381	470.391	0.08	203	0.84	0
269	470.101	N130	58.2	470.036	470.166	0.08	203	0.87	0
270	470.076	N088	5.6	470.043	470.108	0.273	202.93	0.84	0
271	469.079	N290	1.5	469.068	469.089	0.284	205	0.84	0
272	468.984	N222	10.1	468.925	469.043	0.284	203.91	0.84	0
273	468.53	N041	2.5	468.314	468.745	0.284	203.48	0.85	0
274	468.425	N070	26.3	468.188	468.662	0.331	202	0.84	0
275	468.409	N028	5	468.369	468.449	0.331	202.59	0.85	0
276	468.304	N181	8.5	468.24	468.368	0.284	202	0.85	0.0752
277	468.228	N224	11.6	468.128	468.328	0.284	202	0.84	0
278	465.449	N251	7.2	465.365	465.532	0.329	203	0.81	0
279	464.909	N187	19.1	464.74	465.078	0.282	202.6	0.83	0
280	463.491	N001	11.4	463.406	463.576	0.289	202	0.84	0
281	463.244	N060	21.8	463.108	463.381	0.289	203.06	0.84	0
282	461.069	N159	27	460.809	461.329	0.339	201.21	0.81	0.3442
283	460.657	N161	39.6	460.317	460.998	0.289	202	0.81	0
284	460.579	N250	13.6	460.463	460.694	0.289	202	0.81	0
285	460.296	N324	13.9	460.172	460.42	0.289	202.11	0.82	0
286	460.283	N077	16	460.154	460.411	0.289	202	0.82	0
287	457.688	N188	2.7	457.661	457.715	0.289	201.59	0.78	0
288	457.291	N245	8.3	457.209	457.374	0.289	200	0.76	0
289	456.945	N079	16.1	456.826	457.065	0.289	201	0.77	0
290	455.924	N194	33.3	455.558	456.289	0.342	200.86	0.76	0
291	454.597	N140	25.6	454.386	454.808	0.346	204.84	0.57	0
292	452.395	N193	21.1	452.235	452.556	0.29	213.04	0.54	0
293	443.007	N149	11.5	442.93	443.084	0.277	233.61	0.48	0
294	442.536	N100	29	442.317	442.755	0.278	237.13	0.44	0.045
295	442.485	N092	27.3	442.237	442.734	0.32	236.97	0.42	0
296	442.361	N056	0.4	442.361	442.361	0.318	236.4	0.44	0

RGLDIPv6.2 DIP DATA INTERPRETATION: FRACTURE ANALYSIS

borehole _
zone from 441.000 to 707.000 m
North ref is magnetic
11 Nov 2009

Data is classed into 1 types
3 BHTV_dips

Quality cut-off level: *

Mean well deviation: 0.6°deg to N207.4°

4 small-circles defined

	SEARCH AREA azim	pl	cone	MEAN DIP strike	dip	n	f
1	3.0°	88.0°	32.9°	128°	1°	258	0.97
2	201.0°	31.0°	24.6°	292°	61°	10	0.08
3	46.5°	33.8°	25.4°	130°	48°	10	0.06
4	321.1°	43.6°	17.7°	48°	48°	6	0.03

Total number of data = 284
Number of data unaccounted for = 12

ZONE No.	DEVIATION Dev	Azim	DEPTHS m TOP	BASE	No. DATA	MEAN DIPS and FREQUENCIES Str	Dip	n	f	Str	Dip	n	f	Str	Dip	n	f	Str	Dip	n	f
1	**0.5**	**222.1**	**441.87**	**454.06**	**5**	**33**	**14**	**5**	**0.42**	**0**	**0**	**0**	**0.00**	**0**	**0**	**0**	**0.00**	**0**	**0**	**0**	**0.00**
2	0.8	202.5	454.06	474.58	32	51	4	27	1.32	315	67	1	0.12	117	61	1	0.10	47	50	3	0.23
3	0.9	212.4	474.58	491.26	10	106	6	4	0.24	289	62	5	0.63	120	45	1	0.09	0	0	0	0.00
4	0.9	262.2	491.26	510.51	22	165	8	19	1.00	287	51	2	0.17	0	0	0	0.00	0	0	0	0.00
5	0.9	230.2	510.51	534.88	13	4	5	7	0.29	282	71	1	0.12	127	50	3	0.19	51	46	2	0.12
6	0.7	199.5	534.88	579.78	35	82	2	32	0.71	0	0	0	0.00	0	0	0	0.00	46	43	1	0.03
7	0.4	182.2	579.78	599.67	9	153	6	5	0.25	302	58	1	0.09	158	44	1	0.07	0	0	0	0.00
8	0.5	188.7	599.67	650.35	123	211	2	117	2.31	0	0	0	0.00	153	44	1	0.03	0	0	0	0.00
9	0.4	186.8	650.35	679.21	14	88	10	10	0.35	0	0	0	0.00	127	47	2	0.10	0	0	0	0.00
10	0.6	191.7	679.21	707.01	33	120	1	32	1.15	0	0	0	0.00	127	45	1	0.05	0	0	0	0.00

Deviation data Dh4-Co2

DEPTH	INCL	AZIMUTH
2	0.64	183.17
4	0.6	239.72
6	0.52	269.78
8	0.49	185.08
10	0.42	148.13
12	0.39	29.61
14	0.38	312.81
16	0.37	102.28
18	0.43	147.6
20	0.45	37.22
22	0.47	72.53
24	0.41	320.89
26	0.5	259.56
28	0.58	184.12
30	0.6	245.2
32	0.63	163.29
34	0.66	163.92
36	0.68	126.28
38	0.69	21.26
40	0.74	198.97
42	0.7	102.27
44	0.74	23.86
46	0.84	335.29
48	0.73	218.05
50	0.84	193.04
52	0.95	191.66
54	0.92	300.46
56	0.9	196.65
58	0.71	140.77
60	0.78	111.05
62	0.8	221.15
64	0.68	238.92
66	0.68	173.11
68	0.73	145.76
70	0.76	270.23
72	0.7	157.78
74	0.61	253.33
76	0.68	171.94
78	0.6	161.25
80	0.52	184.75
82	0.4	49.11
84	0.48	118.15
86	0.24	45.12
88	0.23	127.29
90	0.11	151.92
92	0.03	125.9
94	0.03	304.66
96	0.13	259.19
98	0.37	241.87
100	0.35	88.07
102	0.39	53.55
104	0.45	240.62
106	0.5	287.3
108	0.68	144.19
110	0.74	130.51
112	0.77	42.78
114	0.69	211.5
116	0.8	259.93
118	0.89	106.43
120	0.78	26.76
122	0.81	300.95
124	0.83	151.92
126	0.77	255.27
128	0.73	34.3
130	0.78	198.39
132	0.83	166.71
134	0.8	26.05
136	0.77	114.88
138	0.86	129.35
140	0.78	78.93

142	0.72	23.5
144	0.68	268.05
146	0.68	76.5
148	0.7	136.71
150	0.61	308.45
152	0.57	70.15
154	0.57	111.08
156	0.6	87.67
158	0.54	175.86
160	0.59	228.75
162	0.67	180.09
164	0.66	218.43
166	0.71	136.21
168	0.74	214.9
170	0.78	61.25
172	0.78	158.55
174	0.82	199.56
176	0.87	32.86
178	0.85	187.15
180	0.82	283.71
182	0.9	216.05
184	0.92	101.95
186	0.92	80.55
188	0.82	173.85
190	0.9	153.66
192	0.93	170.45
194	0.92	214.05
196	0.87	181.92
198	0.94	112.63
200	0.92	160
202	0.86	25.77
204	0.87	240.22
206	0.84	78.27
208	0.81	123.28
210	0.75	270.87
212	0.75	209.15
214	0.74	87.36
216	0.67	195.34
218	0.69	227.34
220	0.68	94.27
222	0.57	48.85
224	0.53	88.17
226	0.62	145.13
228	0.67	126.83
230	0.71	311.7
232	0.68	169.61
234	0.77	79.89
236	0.81	153.15
238	0.81	59.24
240	0.78	194.12
242	0.82	135.31
244	0.85	141.66
246	0.81	80.76
248	0.8	316.75
250	0.88	148.51
252	0.83	53.45
254	0.81	38.15
256	0.84	179.41
258	0.81	85.59
260	0.75	264.7
262	0.75	156.13
264	0.73	228.19
266	0.67	130.49
268	0.67	74.42
270	0.61	97.57
272	0.62	87.85
274	0.63	144.33
276	0.57	179.45
278	0.47	53.89
280	0.34	308.79
282	0.13	170.48
284	0.21	115.6
286	0.43	243.8
288	0.55	261.14
290	0.74	170.87
292	0.77	158.85
294	0.78	258.35

296	0.84	82.59
298	0.87	227.98
300	0.83	342.45
302	0.88	172.45
304	0.84	116.46
306	0.81	163.74
308	0.87	274.86
310	0.82	267.84
312	0.82	290.61
314	0.81	113.08
316	0.81	118.27
318	0.81	131.95
320	0.83	220.17
322	0.83	219.2
324	0.84	84.75
326	0.82	298.52
328	0.83	247.55
330	0.83	100.15
332	0.85	203.61
334	0.81	112.75
336	0.8	124.95
338	0.75	332.8
340	0.74	60.74
342	0.73	144.12
344	0.67	215.7
346	0.63	147.85
348	0.53	97.55
350	0.42	217.32
352	0.23	176.88
354	0.07	214.85
356	0.35	292.33
358	0.51	232.02
360	0.63	282.19
362	0.69	246.6
364	0.66	84.99
366	0.62	336.05
368	0.66	186.15
370	0.7	145.44
372	0.72	98.53
374	0.72	129.38
376	0.71	255.88
378	0.72	191.07
380	0.77	169.94
382	0.78	139.42
384	0.81	298.15
386	0.9	134.41
388	0.51	173.21
390	0.54	165.2
392	0.54	175.6
394	0.56	222.08
396	0.6	222.15
398	0.62	120.83
400	0.67	232.73
402	0.75	92.3
404	0.76	161.33
406	0.79	116.92
408	0.86	301.45
410	0.87	278.82
412	0.9	133.69
414	0.91	234.38
416	0.9	320.35
418	0.89	47.74
420	0.79	285.02
422	0.81	237.13
424	0.76	330.9
426	0.61	302.62
428	0.66	268.25
430	0.65	318.25
432	0.67	299.31
434	0.64	163.6
436	0.73	114.65
438	0.8	180.44
440	0.85	315.79
442	0.7	190.59
444	0.7	194.24
446	0.63	198.18
448	0.73	195.65

450	0.8	195.54
452	0.85	193.96
454	0.87	194.49
456	0.89	195.55
458	0.91	195.23
460	0.9	194.81
462	0.95	195.35
464	0.93	196.51
466	0.95	198.19
468	0.92	196.44
470	0.93	199.36
472	0.9	198.53
474	0.89	196.84
476	0.76	192.95
478	0.64	199.23
480	0.47	198.78
482	0.33	221.27
484	0.31	255.76
486	0.33	249.61
488	0.39	272.62
490	0.52	280.06
492	0.54	280.19
494	0.57	278.45
496	0.58	279.55
498	0.61	279.45
500	0.65	274.47
502	0.64	277.85
504	0.65	275.25
506	0.66	268.45
508	0.72	228.39
510	0.71	214.65
512	0.73	210.63
514	0.74	208.48
516	0.76	207.84
518	0.77	204.97
520	0.78	201.57
522	0.74	194.15
524	0.71	189.28
526	0.65	184.23
528	0.55	179.29
530	0.45	180.28
532	0.32	183.21
534	0.2	198.68
536	0.17	203.23
538	0.15	199.45
540	0.14	195.31
542	0.12	194.83
544	0.14	186.2
546	0.32	176.75
548	0.43	171
550	0.34	174.48
552	0.25	174.06
554	0.18	175.06
556	0.17	178.85
558	0.13	178.25
560	0.07	195.31
562	0.06	280.86
564	0.16	303.06
566	0.27	302.87
568	0.5	293.12
570	0.61	280.45
572	0.67	218.94
574	0.66	204.58
576	0.67	203.24
578	0.65	206.45
580	0.66	218.98
582	0.66	226.39
584	0.65	224
586	0.66	229.47
588	0.65	240.2
590	0.61	269.51
592	0.61	267.17
594	0.62	262.88
596	0.66	220.63
598	0.66	211.27
600	0.64	194.97
602	0.67	190.75

604	0.67	185.36
606	0.7	181.85
608	0.69	179.15
610	0.7	175.97
612	0.7	172.07
614	0.7	169.27
616	0.68	164.13
618	0.66	159.83
620	0.62	151.24
622	0.54	144.7
624	0.46	140
626	0.33	136.76
628	0.3	131.7
630	0.24	96.52
632	0.13	130.19
634	0.1	302.54
636	0.05	293.07
638	0.09	299.28
640	0.15	293.6
642	0.3	286.2
644	0.31	281.17
646	0.37	269.51
648	0.41	247.25
650	0.42	276.4
652	0.4	273.95
654	0.47	270.11
656	0.53	264.6
658	0.56	240.45
660	0.64	233.51
662	0.68	202.63
664	0.7	177.65
666	0.66	159.58
668	0.71	139.83
670	0.7	154.98
672	0.72	158.59
674	0.66	152.91
676	0.75	168.21
678	0.65	159.57
680	0.65	178.55
682	0.66	185.34
684	0.67	197.22
686	0.63	188.45
688	0.67	171.91
690	0.67	159.09
692	0.67	148.76
694	0.66	142.97
696	0.68	140.25
698	0.66	132.7
700	0.67	128.18
702	0.71	129.51
704	0.63	123.52
706	0.66	126.51
708	0.45	104.36
710	1	118.85